Principles of Fluorescence Spectroscopy
(Ed. Joseph R. Lakowicz,
Kluwer Academic/Plenum Publisher, 2nd Ed.1999)

13

Energy Transfer

Fluorescence resonance energy transfer (FRET) is transfer of the excited-state energy from the initially excited donor (D) to an acceptor (A). The donor molecules typically emit at shorter wavelengths which overlap with the absorption spectrum of the acceptor. Energy transfer occurs without the appearance of a photon and is the result of long-range dipole–dipole interactions between the donor and acceptor. The term resonance energy transfer (RET) is preferred because the process does not involve the appearance of a photon. The rate of energy transfer depends upon the extent of spectral overlap of the emission spectrum of the donor with the absorption spectrum of the acceptor, the quantum yield of the donor, the relative orientation of the donor and acceptor transition dipoles, and the distance between the donor and acceptor molecules. The distance dependence of RET has resulted in its widespread use to measure distances between donors and acceptors.

The most common application of RET is to measure the distances between two sites on a macromolecule. Typically, a protein is covalently labeled with a donor and an acceptor (Figure 13.1). The donor is often a tryptophan residue, but extrinsic donors are also used. If there is a single donor and acceptor, and if the D–A distance does not change during the excited-state lifetime, then the D–A distance can be determined from the efficiency of energy transfer. The transfer efficiency can be determined by steady-state measurements of the extent of donor quenching due to the acceptor.

Resonance energy transfer is also used to study macromolecular systems in which a single D–A distance is not present, such as assemblies of proteins and membranes or unfolded proteins where there is a distribution of D–A distances. The extent of energy transfer can also be influenced by the presence of donor-to-acceptor diffusion during the donor lifetime. Although information can be obtained from the steady-state data, such systems are usually studied using time-resolved measurements. These more advanced applications of RET are presented in Chapters 14 and 15.

An important characteristic of energy transfer is that it occurs over distances comparable to the dimensions of biological macromolecules. The distance at which RET is 50% efficient, called the Förster distance,[1] is typically in the range of 20–60 Å. The rate of energy transfer from a donor to an acceptor (k_T) is given by

$$k_T = \frac{1}{\tau_D}\left(\frac{R_0}{r}\right)^6 \qquad [13.1]$$

where τ_D is the decay time of the donor in the absence of acceptor, R_0 is the Förster distance, and r is the donor-to-acceptor (D–A) distance. Hence, the rate of transfer is equal to the decay rate of the donor in the absence of acceptor ($1/\tau_D$) when the D–A distance (r) is equal to the Förster distance (R_0). When the D–A distance is equal to the Förster distance ($r = R_0$), then the transfer efficiency is 50%. At this distance ($r = R_0$), the donor emission would be decreased to one-half of its intensity in the absence of acceptor. The rate of RET depends strongly on distance, being inversely proportional to r^6 (Eq. [13.1]).

Förster distances ranging from 20 to 90 Å are convenient for studies of biological macromolecules. These distances are comparable to the diameter of many proteins, the thickness of biological membranes, and the distance between sites on multisubunit proteins. Any phenomenon which affects the D–A distance will affect the transfer rate, allowing the phenomenon to be quantified. Energy-transfer measurements have been used to estimate the distances between sites on macromolecules and the effects of conformational changes on these distances. In this type of application, one uses the extent of energy transfer between a fixed donor and acceptor to calculate the D–A distance and thus obtain structural information about the macromolecule (Figure 13.1). Such distance measurements have resulted in the description of RET as a "spectroscopic ruler."[2,3] For instance, energy transfer can be used to

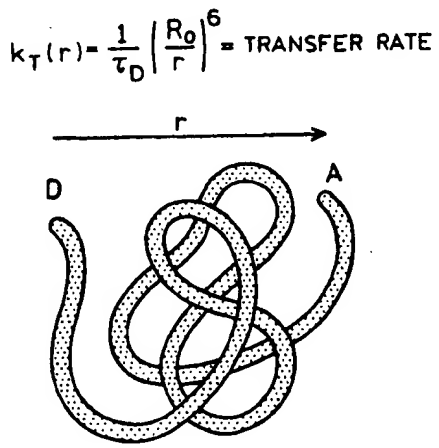

Figure 13.1. Fluorescence resonance energy transfer for a protein with a single donor (D) and a single acceptor (A).

measure the distance from a tryptophan residue to a ligand binding site when the ligand serves as the acceptor.

In the case of multidomain proteins, RET has been used to measure conformational changes which move the domains closer or further apart. Energy transfer can also be used to measure the distance between a site on a protein and a membrane surface, association between protein subunits, and lateral association of membrane-bound proteins. In the case of macromolecular association reactions, one relies less on determination of a precise D–A distance, and more on the simple fact that energy transfer occurs whenever the donors and acceptors are in close proximity comparable to the Förster distance.

The use of energy transfer as a proximity indicator illustrates an important characteristic of energy transfer. Energy transfer can be reliably assumed to occur whenever the donors and acceptors are within the characteristic Förster distance, and whenever suitable spectral overlap occurs. The value of R_0 can be reliably predicted from the spectral properties of the donors and acceptors. Energy transfer is a through-space interaction which is mostly independent of the intervening solvent and/or macromolecule. In principle, the orientation of the donors and acceptors can prevent energy transfer between a closely spaced D–A pair, but such a result is rare, and possibly nonexistent in biomolecules. Hence, one can assume that RET will occur if the spectral properties are suitable and the D–A distance is comparable to R_0. A wide variety of biochemical interactions result in changes in distance and are thus measurable using RET.

RET is a process which does not involve emission and reabsorption of photons. The theory of energy transfer is based on the concept of a fluorophore as an oscillating dipole, which can exchange energy with another dipole with a similar resonance frequency.[4] Hence, RET is similar to the behavior of coupled oscillators, like two swings on a common supporting beam. In contrast, radiative energy transfer is due to emission and reabsorption of photons and is thus due to inner filter effects. Radiative transfer depends upon less interesting optical properties of the sample, such as the size of the sample container, the path length, the optical densities of the sample at the excitation and emission wavelengths, and the geometric arrangement of the excitation and emission light paths. In contrast, nonradiative energy transfer contains a wealth of structural information concerning the donor–acceptor pair.

RET contains molecular information which is different from that revealed by solvent relaxation, excited-state reactions, fluorescence quenching, or fluorescence anisotropy. These other fluorescence phenomena depend on interactions of the fluorophore with other molecules in the surrounding solvent shell. These nearby interactions are less important for energy transfer, except for their effects on the spectral properties of the donor and acceptor. Nonradiative energy transfer is effective over much longer distances, and the intervening solvent or macromolecule has little effect on the efficiency of energy transfer, which depends primarily on the D–A distance. In this chapter we will describe the basic theory of nonradiative energy transfer. This theory is applicable to a D–A pair separated by a fixed distance, but we also describe examples of RET from membrane-bound proteins to randomly distributed lipid acceptors and the use of RET to study association reactions. More complex formalisms are needed to describe other commonly encountered situations, such as distance distributions (Chapter 14) and the presence of multiple acceptors (Chapter 15).

13.1. THEORY OF ENERGY TRANSFER FOR A DONOR–ACCEPTOR PAIR

The theory for RET is moderately complex, and similar equations have been derived from classical and quantum-mechanical considerations. We will describe only the final equations. Readers interested in the physical basis of RET are referred to the excellent review by Clegg.[4] RET is best understood by considering a single donor and acceptor separated by a distance r. The rate of transfer for a donor and acceptor separated by a distance r is given by

$$k_T(r) = \frac{Q_D \kappa^2}{\tau_D r^6}\left(\frac{9000\ (\ln 10)}{128\ \pi^5 N n^4}\right)\int_0^\infty F_D(\lambda)\epsilon_A(\lambda)\lambda^4\, d\lambda \qquad [13.2]$$

where Q_D is the quantum yield of the donor in the absence of acceptor; n is the refractive index of the medium, which

is typically assumed to be 1.4 for biomolecules in aqueous solution; N is Avogadro's number; τ_D is the lifetime of the donor in the absence of acceptor; $F_D(\lambda)$ is the corrected fluorescence intensity of the donor in the wavelength range λ to $\lambda + \Delta\lambda$, with the total intensity (area under the curve) normalized to unity; $\varepsilon_a(\lambda)$ is the extinction coefficient of the acceptor at λ, which is typically in units of M^{-1} cm^{-1}; κ^2 is a factor describing the relative orientation in space of the transition dipoles of the donor and acceptor and is usually assumed to be equal to $\frac{2}{3}$, which is appropriate for dynamic random averaging of the donor and acceptor (see Section 13.1.A below). In Eq. [13.2] we wrote the transfer rate k_T as a function of r, $k_T(r)$, to emphasize its dependence on distance.

The overlap integral $J(\lambda)$ expresses the degree of spectral overlap between the donor emission and the acceptor absorption,

$$J(\lambda) = \int_0^\infty F_D(\lambda)\varepsilon_A(\lambda)\lambda^4\, d\lambda = \frac{\int_0^\infty F_D(\lambda)\varepsilon_A(\lambda)\lambda^4\, d\lambda}{\int_0^\infty F_D(\lambda)\, d\lambda} \qquad [13.3]$$

$F_D(\lambda)$ is dimensionless. If $\varepsilon_A(\lambda)$ is expressed in units of M^{-1} cm^{-1} and λ is in nanometers, then $J(\lambda)$ is in units of M^{-1} cm^{-1} nm^4. If λ is in centimeters, then $J(\lambda)$ is in units of M^{-1} cm^3. In calculating $J(\lambda)$, one should use the corrected emission spectrum with its area normalized to unity (Eq. [13.3], middle) or normalize the calculated value of $J(\lambda)$ by the area (Eq. [13.3], right). The overlap integral has been defined in several ways, each with different units. In our experience, we find that it is easy to get confused so we recommend the units of nanometers or centimeters for the wavelength and units of M^{-1} cm^{-1} for the extinction coefficient.

Because the transfer rate $k_T(r)$ depends on r, it is inconvenient to use this rate constant in the design of biochemical experiments. For this reason, Eq. [13.2] is written in terms of the Förster distance R_0, at which the transfer rate $k_T(r)$ is equal to the decay rate of the donor in the absence of acceptor (τ_D^{-1}). At this distance, one-half of the donor molecules decay by energy transfer and one-half decay by the usual radiative and nonradiative rates. From Eqs. [13.1] and [13.2] with $k_T(r) = \tau_D^{-1}$, one obtains

$$R_0^6 = \frac{9000(\ln 10)\kappa^2 Q_D}{128\,\pi^5 N n^4} \int_0^\infty F_D(\lambda)\varepsilon_A(\lambda)\lambda^4\, d\lambda \qquad [13.4]$$

This expression allows the Förster distance to be calculated from the spectral properties of the donor and the acceptor and the donor quantum yield. While Eq. [13.4] looks complex, many of the terms are simple physical constants. It is convenient to have simpler expressions for R_0 in terms of the experimentally known values, which is accomplished by combining the constant terms in Eq. [13.4]. If the wavelength is expressed in nanometers, then $J(\lambda)$ is in units of M^{-1} cm^{-1} (nm)^4 and the Förster distance, in angstroms, is given by

$$R_0 = 0.211[\kappa^2 n^{-4} Q_D J(\lambda)]^{1/6} \quad \text{(in Å)} \qquad [13.5]$$

and

$$R_0^6 = 8.79 \times 10^{-5}[\kappa^2 n^{-4} Q_D J(\lambda)] \quad \text{(in Å}^6\text{)} \qquad [13.6]$$

If the wavelength is expressed in centimeters and $J(\lambda)$ is in units of M^{-1} cm^3, then the Förster distance is given by

$$R_0^6 = 8.79 \times 10^{-25}[\kappa^2 n^{-4} Q_D J(\lambda)] \quad \text{(in cm}^6\text{)} \qquad [13.7]$$

or

$$R_0 = 9.78 \times 10^3[\kappa^2 n^{-4} Q_D J(\lambda)]^{1/6} \quad \text{(in Å)} \qquad [13.8]$$

and

$$R_0^6 = 8.79 \times 10^{23}[\kappa^2 n^{-4} Q_D J(\lambda)] \quad \text{(in Å}^6\text{)} \qquad [13.9]$$

It is important to recognize that the Förster distances are usually reported for an assumed value of κ^2, typically $\kappa^2 = \frac{2}{3}$. Once the value of R_0 is known, the rate of energy transfer can be easily calculated using

$$k_T(r) = \frac{1}{\tau_D}\left(\frac{R_0}{r}\right)^6 \qquad [13.10]$$

One can then readily determine whether the rate of transfer will be competitive with the decay rate (τ_D^{-1}) of the donor. If the transfer rate is much faster than the decay rate, then energy transfer will be efficient. If the transfer rate is slower than the decay rate, then little transfer will occur during the excited-state lifetime, and RET will be inefficient.

The efficiency of energy transfer (E) is the fraction of photons absorbed by the donor that are transferred to the acceptor. This fraction is given by

$$E = \frac{k_T}{\tau_D^{-1} + k_T} \qquad [13.11]$$

which is the ratio of the transfer rate to the total decay rate of the donor. Recalling that $k_T = \tau_D^{-1}(R_0/r)^6$, one can easily rearrange Eq. [13.11] to yield

$$E = \frac{R_0^6}{R_0^6 + r^6} \qquad [13.12]$$

This equation shows that the transfer efficiency is strongly dependent on distance when the D–A distance is near R_0 (Figure 13.2). The efficiency quickly increases to 1.0 as the D–A distance decreases below R_0. For instance, if $r = 0.1R_0$, one can readily calculate that the transfer efficiency is 0.999999, so that the donor emission would not be observable. Conversely, the transfer efficiency quickly decreases to zero if r is greater than R_0. Because E depends so strongly on distance, measurements of the distance (r) are only reliable when r is within a factor of 2 of R_0 (see Problem 13.7). If r is twice the Förster distance ($r = 2R_0$), then the transfer efficiency is 1.56%.

The transfer efficiency is typically measured using the relative fluorescence intensity of the donor, in the absence (F_D) and presence (F_{DA}) of acceptor. The transfer efficiency can also be calculated from the lifetimes under these respective conditions (τ_D and τ_{DA}):

$$E = 1 - \frac{\tau_{DA}}{\tau_D} \qquad [13.13]$$

$$E = 1 - \frac{F_{DA}}{F_D} \qquad [13.14]$$

It is important to remember the assumptions involved in the derivation of these equations. Equations [13.13] and [13.14] are only applicable to donor–acceptor pairs which are separated by a fixed distance. This situation is frequently encountered for labeled proteins. However, a single fixed donor–acceptor distance is not found for a mixture of donors and acceptors in solution, nor for donors and acceptors dispersed randomly in membranes. More complex expressions are required in these cases, and such expressions are generally derived by averaging the transfer rate over the assumed spatial distribution of donor–acceptor pairs.[5]

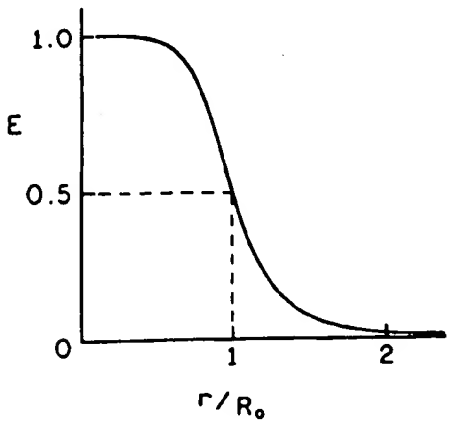

Figure 13.2. Dependence of the energy transfer efficiency (E) on distance. R_0 is the Förster distance.

The use of lifetimes in Eq. [13.13] has been a source of confusion. In Eq. [13.13] we have assumed that the decay of the donor is a single exponential in the absence (τ_D) and presence (τ_{DA}) of acceptor. Single-exponential decays are rare in biomolecules. If the intensity decays are multiexponential, then it is important to use average decay times in Eq. [13.13] which are proportional to the steady-state intensities. These averages are given by the sum of the $\alpha_i\tau_i$ products. Also, even if the donor decay is a single exponential, the decay rate in the presence of acceptor will only remain a single exponential if there is a single D–A distance. The presence of acceptors at more than one distance can result in more complex decays (Chapter 14).

Assuming that the single-distance model is appropriate, one sees that the rate of energy transfer is dependent upon R_0, which in turn depends upon κ^2, n, Q_D, and $J(\lambda)$. These factors must be known in order to calculate the distance. The refractive index is generally known from the solvent composition or is estimated for the macromolecule. The refractive index is often assumed to be close to that of water (n = 1.33) or small organic molecules (n = 1.39). The quantum yield of the donor, Q_D, is determined by comparison with standard fluorophores. Since Q_D is used as the sixth root in the calculation of R_0, small errors in Q_D do not have a large effect on R_0. The overlap integral must be evaluated for each D–A pair. The greater the overlap of the emission spectrum of the donor with the absorption spectrum of the acceptor, the higher is the value of R_0. Acceptors with larger extinction coefficients result in larger R_0 values. In the equations presented above, it was assumed that the lifetime of the donor was not altered by binding of the acceptor, other than by the rate of energy transfer. For labeled macromolecules, this may not always be the case. Allosteric interactions between the donor and acceptor sites could alter the donor lifetime by enhancement of other decay processes, or by protection from these processes. Under these circumstances, more complex analysis of the apparent transfer efficiency is required, typically by a comparison of the apparent efficiency by donor quenching and enhanced acceptor emission (Section 13.3.D).

The dependence of R_0 on spectral overlap is illustrated in Figure 13.3 for RET from structural isomers of dansyl-labeled phosphatidylethanolamine (DPE) to the eosin-labeled lipid (EPE). Each of the dansyl derivatives of DPE displays a different emission spectrum.[5] As the spectra of the DPE isomers shift to longer wavelengths, the overlap

with the absorption spectrum of EPE increases and the R_0 values increase (Table 13.1). One notices that R_0 is not very dependent upon $J(\lambda)$. For instance, for two of the D–A pairs, a 120-fold change in the overlap integral results in a 2.2-fold change in the Förster distance. This is because of the sixth-root dependence in Eq. [13.5]. It should also be noted that the visual impression of overlap is somewhat misleading because the value of $J(\lambda)$ depends on λ^4 (Eq. [13.3]). Comparison of the spectral overlap for 2,5-DPE and 1,5-DPE suggests a larger Förster distance for 1,5-DPE, whereas the calculated value is smaller. The larger Förster distance for 2,5-DPE is due to its larger quantum yield.

Because of the complexity in calculating overlap integrals and Förster distances, it is convenient to have several examples. Values of the overlap integral corresponding to the spectra in Figure 13.3 are summarized in Table 13.1.

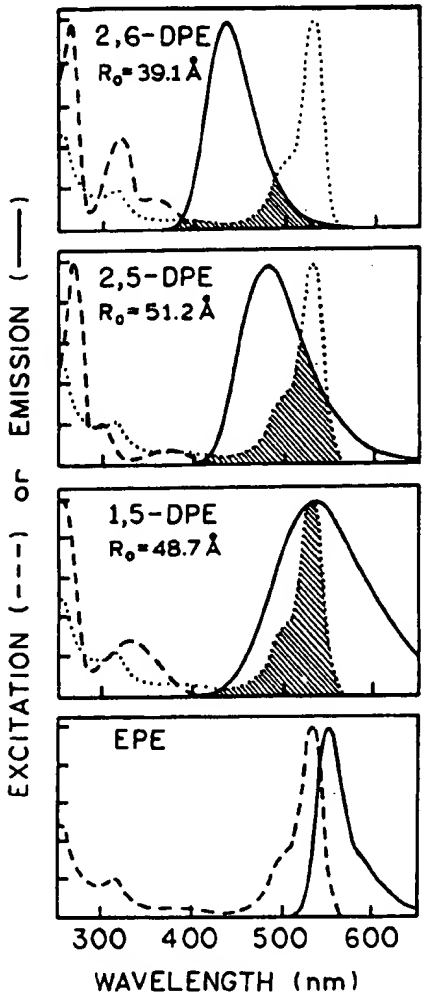

Figure 13.3. Excitation (---) and emission (—) spectra of dansyl-labeled lipids and an eosin-labeled lipid. The eosin- and dansyl-labeled compounds are N-derivatives of phosphatidylethanolamine (PE). In the designations of the dansyl-PE (DPE) derivatives, the numbers refer to the location of the dimethylamino and sulfonyl residues on the naphthalene ring of the dansyl group. The extinction coefficient of eosin-PE (EPE) is 85,000 M^{-1} cm^{-1} at 527 nm. In the top three panels, the long-wavelength absorption spectrum of eosin-PE is shown as a dotted curve. Revised from Ref. 5.

Brief Biographical Sketch of Theodor Förster

The theory for resonance energy transfer was developed by Professor Theodor Förster (Figure 13.4). He was born in Frankfurt, Germany, in 1910. He received a Ph.D. in 1933 for studies of the polarization of reflected electrons. He then became a research assistant in Leipzig, Germany, where he studied light absorption of organic compounds until 1942. In this phase of his work, he applied the newly developed principles of quantum mechanics to chemistry. His most productive period followed World War II. From 1942 to 1945, he held a professorship in Poznan, Poland, where he did not appear to publish any papers, but he did get married. In 1945 he joined the Max-Planck Institute for Physical Chemistry in Göttingen, where he wrote his classic book *Fluoreszenz Organischer Verbindungen*, which has been described as a concentrated "house bible" for the German community of spectroscopists. By 1946 Professor Förster had written his first paper on energy transfer and pointed out the importance of energy transfer in photosynthesis systems. Professor Förster was also among the first scientists to observe excited-state proton transfer, which is now described by the Förster cycle. In 1954 he discovered excimer formation. Professor Förster died of a heart attack in his car on the way to work in 1974. (For additional biographical information, see Ref. 6 and the Introduction about Theodor Förster in Ref. 7.)

13.1.A. Orientation Factor κ^2

A final factor in the analysis of the energy-transfer efficiencies is the orientation factor κ^2, which is given by

$$\kappa^2 = (\cos\theta_T - 3\cos\theta_D \cos\theta_A)^2 \qquad [13.15]$$

$$= (\sin\theta_D \sin\theta_A \cos\phi - 2\cos\theta_D \cos\theta_A)^2 \qquad [13.16]$$

In these equations, θ_T is the angle between the emission transition dipole of the donor and the absorption transition

Table 13.1. Calculated R_0 Values for RET from Structural Isomers of Dansyl-Labeled Phosphatidylethanolamine (DPE) to Eosin-Labeled Ethanolamine (EPE) and from 2,6-DPE to 2,5-DPE[a]

Donor	Acceptor	ϕ_D	J (M^{-1} cm^3)	J (M^{-1} cm^3 (nm)^4)[b]	R_0 (Å)
1,5-DPE	EPE	0.37	2.36×10^{-13}	2.36×10^{15}	48.7
2,5-DPE	EPE	0.76	1.54×10^{-13}	1.54×10^{15}	51.2
2,6-DPE	EPE	0.71	3.31×10^{-14}	3.31×10^{14}	39.1
2,6-DPE	2,5-DPE	0.71	1.3×10^{-15}	1.3×10^{13}	22.8

[a]From Ref. 5. R_0 was calculated using $n = 1.4$ and $\kappa^2 = \frac{2}{3}$.
[b]The factor of 10^{28} between $J(\lambda)$ in M^{-1} cm^3 and M^{-1} cm^3 nm^4 arises from 1 nm = 10^{-7} cm, raised to the fourth power.

dipole of the acceptor, θ_D and θ_A are the angles between these dipoles and the vector joining the donor and the acceptor, and ϕ is the angle between the planes (Figure 13.5). Depending upon the relative orientation of donor and acceptor, κ^2 can range from 0 to 4. For collinear and parallel transition dipoles, $\kappa^2 = 4$, and for parallel dipoles, $\kappa^2 = 1$. Since the sixth root of κ^2 is taken in calculating the distance, variation of κ^2 from 1 to 4 results in only a 26% change in r. With $\kappa^2 = \frac{2}{3}$, as is usually assumed, the calculated distance can be in error by no more than 35%. However, if the dipoles are oriented perpendicular to one another, $\kappa^2 = 0$, which would result in serious errors in the calculated distance. This problem has been discussed in detail.[8–10] By measurements of the fluorescence anisotropy of the donor and the acceptor, one can set limits on κ^2 and thereby minimize uncertainties in the calculated distance.[9–11] An example of calculating the range of possible values of κ^2 is given in Section 13.2.B. In general, variation of κ^2 seems to have not resulted in major errors in the calculated distances.[12,13] Generally, κ^2 is assumed equal to $\frac{2}{3}$, which is the value for donors and acceptors that randomize by rotational diffusion prior to energy transfer. This value is generally assumed for calculation of R_0. Alternatively, one may assume that a range of static donor—acceptor orientations are present and that these orientations do not change during the lifetime of the excited state. In this case, $\kappa^2 = 0.476$.[3] For fluorophores bound to macromolecules, segmental motions of the donor and acceptor tend to randomize the orientations. Further, many

Figure 13.4. Professor Theodor Förster, May 15, 1910–May 20, 1974. Reprinted, with permission, from Ref. 6, Copyright © 1974, Springer-Verlag.

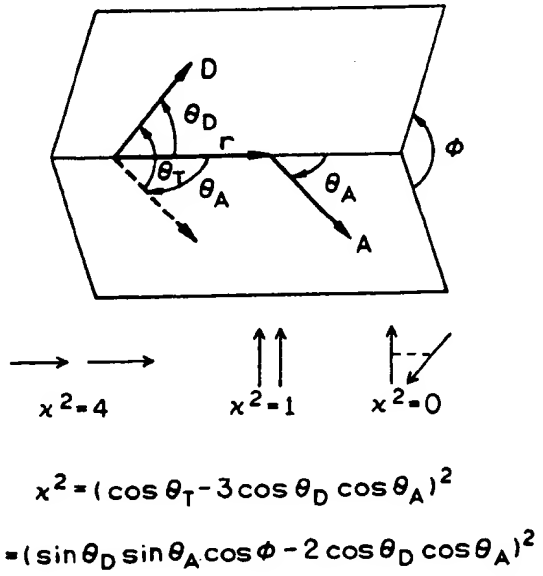

Figure 13.5. Dependence of the orientation factor κ^2 on the directions of the emission dipole of the donor and the absorption dipole of the acceptor.

donors and acceptors display fundamental anisotropies less than 0.4 owing to overlapping electronic transitions. In this case, the range of possible κ^2 values is more limited, and errors in distance are likely to be less than 10%.[14]

13.1.B. Dependence of the Transfer Rate on Distance (r), the Overlap Integral (J), and κ^2

The theory of Förster predicts that $k_T(r)$ depends on $1/r^6$ (Eq. [13.1]) and linearly on the overlap integral (Eq. [13.2]). Given the complexity and assumptions of RET theory,[4] it was important to demonstrate experimentally that these dependencies are valid. The predicted $1/r^6$ dependence on distance was confirmed experimentally.[15–17] One demonstration used oligomers of poly-L-proline, labeled on opposite ends with a naphthyl (donor) and a dansyl (acceptor) group.[15,16] Poly-L-proline forms a rigid helix of known atomic dimensions, providing fixed distances between the donor and acceptor moieties. By measuring the transfer efficiency with different numbers of proline residues, it was possible to demonstrate that the transfer efficiency in fact decreased as $1/r^6$. These data are described in detail in Problem 13.3.

The linear dependence of k_T on the overlap integral J has also been experimentally proven.[18] This was accomplished using a D–A pair linked by a rigid steroid spacer. The extent of spectral overlap was altered by changing the solvent, which shifted the indole donor emission spectrum and the carbonyl acceptor absorption spectrum. The rate of transfer was found to decrease linearly as the overlap integral decreased. These data are shown in Problem 13.4. To date, there has not been experimental confirmation of the dependence of the transfer rate on κ^2.

Another important characteristic of RET is that the transfer rate is proportional to the decay rate of the fluorophore (Eq. [13.1]). This means that for a D–A pair spaced by the R_0 value, the rate of transfer will be $k_T = \tau_D^{-1}$ whether the decay time is 10 ns or 10 ms. Hence, long-lived lanthanides are expected to display RET over distances comparable to those for the nanosecond-decay-time fluorophores, as demonstrated by transfer from Tb^{3+} to Co^{2+} in thermolysin.[19] This fortunate result occurs because the transfer rate is proportional to the emission rate of the donor. The proportionality to the emissive rate is due to the term Q_D/τ_D in Eq. [13.2]. It is interesting to speculate what would happen if the transfer rate were independent of the decay rate. In this case, a longer-lived donor would allow more time for energy transfer. Then energy transfer would occur over longer distances where the smaller rate of transfer would still be comparable to the donor decay rate.

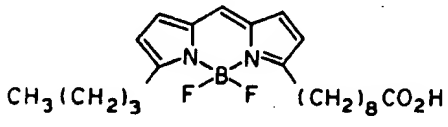

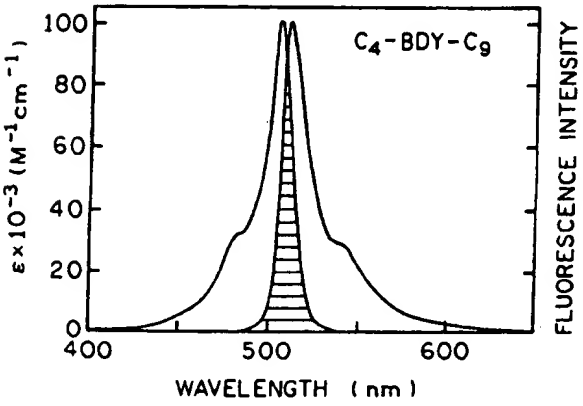

Figure 13.6. Absorption and corrected fluorescence emission (bandpass 2.5 nm) spectra of the BODIPY derivative C_4-BDY-C_9 in methanol, with shaded area representing spectral overlap. Revised and reprinted, with permission, from Ref. 20, Copyright © 1991, Academic Press, Inc.

13.1.C. Homotransfer and Heterotransfer

In the preceding sections we considered only energy transfer between chemically distinct donors and acceptors, which is called heterotransfer. RET can also occur between chemically identical molecules. Such transfer, termed homotransfer, typically occurs for fluorophores which display small Stokes' shifts. One example of homotransfer is provided by the relatively new class of fluorophores referred to as BODIPY* dyes.[20] The absorption and emission spectra of one BODIPY derivative are shown in Figure 13.6. Because of the small Stokes' shift and high extinction coefficient of these probes, the Förster distance for homotransfer is near 57 Å.[20]

At first glance, homotransfer may seem like an unlikely phenomenon, but its occurrence is rather common. For example, it is well known that antibodies labeled with fluorescein do not become more highly fluorescent with higher degrees of labeling.[21] Antibodies are typically brightest with about four fluoresceins per antibody, after which the intensity starts to decrease. This effect is attributed to the small Stokes' shift of fluorescence and homotransfer. In fact, homotransfer among fluorescent molecules was one of the earliest observations in fluores-

*BODIPY, 4,4-difluoro-4-bora-3a,4a-diaza-s-indacene. BODIPY is a trademark of Molecular Probes, Inc.

cence and was detected by a decrease in the anisotropy of fluorophores at higher concentrations.[22] The possibility of homotransfer can be readily evaluated by examination of the absorption and emission spectra. For instance, perylene would be expected to display homotransfer, but homotransfer is unlikely for quinine (Figure 1.3).

13.2. DISTANCE MEASUREMENTS USING RET

13.2.A. Distance Measurements in α-Helical Melittin

Because RET can be reliably assumed to depend on $1/r^6$, the transfer efficiency can be used to measure distances between sites in proteins. This use of energy transfer has been recently summarized in useful reviews.[12,23] These articles contain R_0 values for a number of commonly used D–A pairs and offer practical advice. The use of RET in structural biochemistry is illustrated in Figure 13.7 for the peptide melittin.[24] This peptide has 26 amino acids. A single tryptophan residue at position 19 serves as the donor. A single dansyl acceptor was placed on the N-terminal amino group. The spectral properties of this D–A pair are shown in Figure 13.8. These spectral properties result in a Förster distance of 23.6 Å (Problem 13.5).

Depending upon the solvent conditions, melittin can exist in the monomer, tetramer, α-helix, and/or random-coil state.[25–27] In the methanol–water mixture specified on Figure 13.7, melittin is in the rigid α-helical state and exists as a monomer. There is a single dansyl acceptor adjacent to each tryptophan donor, and the helical structure ensures a single D–A distance. Hence, we can use the theory

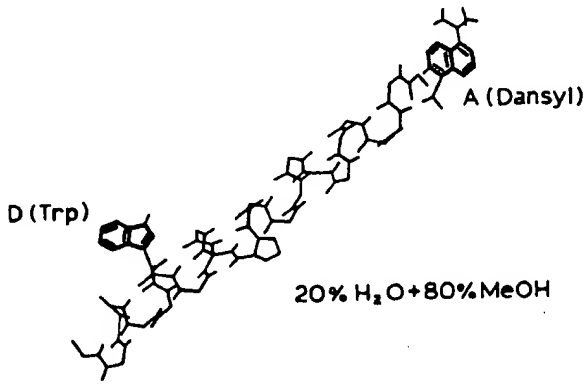

Figure 13.7. Structure of melittin in the α-helical state. The donor is tryptophan-19, and the acceptor is an N-terminal dansyl group. Revised from Ref. 24.

described above, and in particular Eqs. [13.12] and [13.14], to calculate the D–A distance.

In order to calculate the D–A distance, it is necessary to determine the efficiency of energy transfer. This can only be accomplished by comparing the intensity of the donor in the presence of acceptor (F_{DA}) with the donor intensity from a control molecule which lacks the acceptor (F_D). From Figure 13.9 one sees that the value of F_{DA}/F_D is near 0.55, so that the transfer efficiency is less than 50% (E = 0.45). Since E is less than 0.5, we know that the D–A distance must be larger than the R_0 value. Using Eq. [13.12], and the R_0 value of 23.6 Å, one can readily calculate that the tryptophan-to-dansyl distance is 24.4 Å.

It is important to notice the assumptions used in calculating the distance. We assumed that the orientation factor κ^2 was equal to the dynamic average of $\frac{2}{3}$. In the case of melittin, this is a good assumption because both the trp

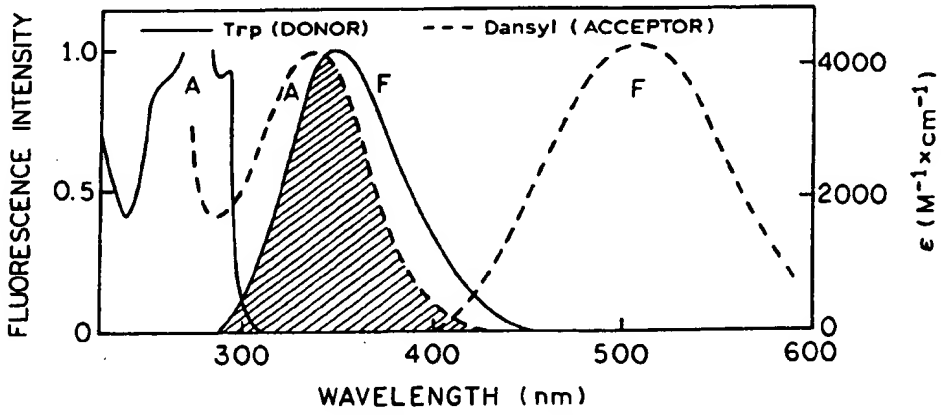

Figure 13.8. Overlap integral (shaded area) for energy transfer from a tryptophan donor to a dansyl acceptor on melittin. R_0 = 23.6 Å. Data from Ref. 24.

nor and dansyl acceptor are fully exposed to the liquid ase, which is highly fluid. The rotational correlation ıes for such groups are typically near 100 ps, so that the ɔoles can randomize during the excited-state lifetime. rhaps the most dangerous assumption is that the sample 100% labeled with acceptor. If melittin were incom-:tely labeled with acceptor, the measured value of F_{DA} ıuld be larger than the true value, and the calculated tance too large. Suppose that the fractional labeling with :eptor is given by f_A, so that the fractional donor popu-ion lacking acceptor is given by $1 - f_A$. In this case, Eq. 3.14] becomes[11]

$$E = 1 - \frac{F_{DA} - F_D(1 - f_A)}{F_D f_A} = \left(1 - \frac{F_{DA}}{F_D}\right)\frac{1}{f_A} \qquad [13.17]$$

r a high degree of RET donor quenching ($F_{DA}/F_D \ll 1$), mall percentage of unlabeled acceptor can result in a ge change in the calculated transfer efficiency (Problem .9).

Another assumption in calculating the trp to dansyl tance in melittin is that a single conformation exists, i.e., t there is a single D–A distance. This assumption is ɔbably safe for many proteins in the native state, particu-ly for single-domain proteins. For unfolded peptides or ıltidomain proteins, a variety of conformations can exist, ulting in a range of D–A distances. In this case, calcu-on of a single distance using Eq. [13.12] would result an apparent distance, which would be weighted toward shorter distances. Such systems are best analyzed in ms of a distance distribution (Chapter 14).

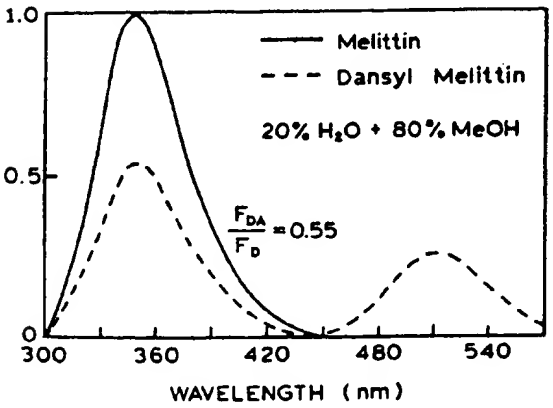

ıre 13.9. Emission spectra of the melittin donor (D) and acceptor-led melittin (D–A). Excitation at 282 nm. Revised from Ref. 24.

13.2.B. Effect of κ^2 on the Possible Range of Distances

In distance measurements using RET, there is often concern about the effects of the orientation factor κ^2. At present, there is no way to measure κ^2, short of determination of the X-ray crystal structure, in which case the distance would be known and thus there would be no reason to use energy transfer. However, it is possible to set limits on κ^2, which in turn sets limits on the range of possible D–A distances. These limits are determined from the anisotropies of the donor and acceptor, which reflect the extent of orientational averaging toward the dynamic average of $\kappa^2 = \frac{2}{3}$.

The problem of κ^2 has been discussed in detail by Dale and co-workers[8–10] and summarized by Cheung.[11] The basic idea is that the donor and acceptor move freely within a cone and that energy transfer is rapidly averaged over all available D–A orientations. Interpretation of the formalism described by Dale and co-workers[8–10] is not always straightforward, and we present the method preferred in our laboratory.[28] Although it is not possible to calculate the values of κ^2, it is possible to set upper and lower limits. These values are given by

$$\kappa^2_{min} = \frac{2}{3}\left[1 - \frac{(d^x_D + d^x_A)}{2}\right] \qquad [13.18]$$

$$\kappa^2_{max} = \frac{2}{3}(1 + d^x_D + d^x_A + 3d^x_D d^x_A) \qquad [13.19]$$

where

$$d^x_i = \left(\frac{r_i}{r_0}\right)^{1/2} \qquad [13.20]$$

The value of d^x_i represents the depolarization factor due to segmental motion of the donor (d^x_D) or acceptor (d^x_A), but not the depolarization due to overall rotational diffusion of the protein. Overall rotational diffusion is not important because it does not change the D–A orientation. The values of r_i and r_0 are often taken as the steady-state and fundamental anisotropies, respectively, of the donor or acceptor. If the donor and acceptor do not rotate relative to each other during the excited-state lifetime, then $d^x_D = d^x_A = 1.0$, and $\kappa^2_{min} = 0$ and $\kappa^2_{max} = 4$. If both D and A are independently and rapidly rotating over all space, $\kappa^2_{min} = \kappa^2_{max} = \frac{2}{3}$.

There are several ways to obtain the values of d^x_D and d^x_A. The easiest method is to determine the anisotropy decays of the donor and acceptor, the latter when directly excited. This calculation of a range of κ^2 values is illustrated by the anisotropy decays measured for the trypto-

phan donor and dansyl acceptor in α-helical melittin (Table 13.2). Both the donor and the acceptor display two correlation times, one near 2 ns due to overall protein rotation, and a shorter correlation time near 0.3 ns due to segmental motions of the donor and the acceptor. It is these faster motions which randomize κ^2. The values of d_D^x and d_A^x are given by the ratio of the long-correlation-time amplitude to the total anisotropy. Hence, for melittin,

$$d_D^x = \left(\frac{0.174}{0.294}\right)^{1/2} = 0.77 \qquad [13.21]$$

$$d_A^x = \left(\frac{0.135}{0.300}\right)^{1/2} = 0.67 \qquad [13.22]$$

Using these values and Eqs. [13.18] and [13.19], one can calculate the limits on κ^2, $\kappa^2_{min} = 0.19$ and $\kappa^2_{max} = 2.66$.

Once the limiting values of κ^2 are known, one may use these values to calculate the maximum and minimum values of the distance that are consistent with the data. In calculating these distances, one must remember that R_0 was calculated with an assumed value of $\kappa^2 = \frac{2}{3}$. Hence, the minimum and maximum distances are given by

$$r_{min} = \left(\frac{\kappa^2_{min}}{2/3}\right)^{1/6} r\left(\frac{2}{3}\right) \qquad [13.23]$$

$$r_{max} = \left(\frac{\kappa^2_{max}}{2/3}\right)^{1/6} r\left(\frac{2}{3}\right) \qquad [13.24]$$

where $r(\frac{2}{3})$ is the distance calculated assuming $\kappa^2 = \frac{2}{3}$. Using the limiting values of κ^2, one finds for the example given above that the distance can be from 0.81 to 1.26 of $r(\frac{2}{3})$, the distance calculated with the assumed value of $\kappa^2 = \frac{2}{3}$. While this range may seem large, it should be remembered that there is an additional depolarization factor due to the transfer process itself, which will further randomize κ^2 toward $\frac{2}{3}$. Equations [13.18]–[13.20] provide a worst-case estimate, which usually overestimates the effects of κ^2 on the calculated distance. For fluorophores with mixed polarization, $r_0 < 0.3$, the error in distance is thought to be below 10%.[14]

Table 13.2. Anisotropy Decays for α-Helical Melittin[a]

Fluorophore	r_{0i}	ϕ_i (ns)
Tryptophan-19[b]	0.120	0.23
	0.174	1.77
N-terminal dansyl	0.165	0.28
	0.135	2.18

[a]From Ref. 24.

[b]Determined for donor-only melittin. Similar amplitudes and correlation times were found for trp-19 in dansyl-melittin.

There are two other ways to obtain the depolarization factors. One method is to construct a Perrin plot in which the steady-state polarization is measured for various viscosities. Upon extrapolation to the high-viscosity limit, the $1/r_0^{app}$ intercept (Section 10.5) is typically larger than $1/r_0$ in frozen solution. This difference is usually attributed to segmental probe motions and can be used to estimate the depolarization factor, $d_i^x = (r_0^{app}/r_0)^{1/2}$. Another method is to estimate the expected steady-state anisotropy from the lifetime and correlation time of the protein and to use these data to estimate d_D^x and d_A^x (Problem 13.8). The basic idea is to estimate d_A^x and d_D^x by correcting for the decrease in anisotropy resulting from rotational diffusion of the protein. Any loss in anisotropy, beyond that calculated for overall rotation, is assumed to be due to segmental motions of the donor or acceptor.

13.2.C. Protein Folding Measured by RET

Energy transfer has also been widely useful for measurements of protein folding. One example is for the protein serine hydroxymethyltransferase. This protein typically has three tryptophan residues, at positions 16, 183, and 385.[29] The acceptor was a pyridoxyl 5′-phosphate (PyP) residue covalently linked to lysine-229. One expects protein folding or unfolding to affect the distance from each of the tryptophan residues to PyP, and thus one expects the extent of RET to be different for the native and folded proteins.

The presence of three tryptophan residues results in emission from three donors, which would be practically impossible to interpret. For this reason, single-tryptophan mutants were prepared which each lacked the other two trp residues. This procedure results in a single trp–PyP pair for each mutant protein. Emission spectra are shown for the trp-183 mutant in Figure 13.10. The protein was initially in 8*M* urea, resulting in a random-coil state; the initial emission spectrum is shown as the dashed curve in Figure 13.10. Upon dilution into buffer without urea, the protein began to refold, as seen by a decrease in the trp-donor emission and an increase in the PyP-acceptor emission. The intensity of the PyP emission increases upon refolding due to increased RET from trp-183. (Enhancement of acceptor emission is described in more detail in Section 13.3.D.) The availability of three single-tryptophan mutants allowed studies of refolding of specific sites on the protein. The PyP acceptor emission at 380 nm was

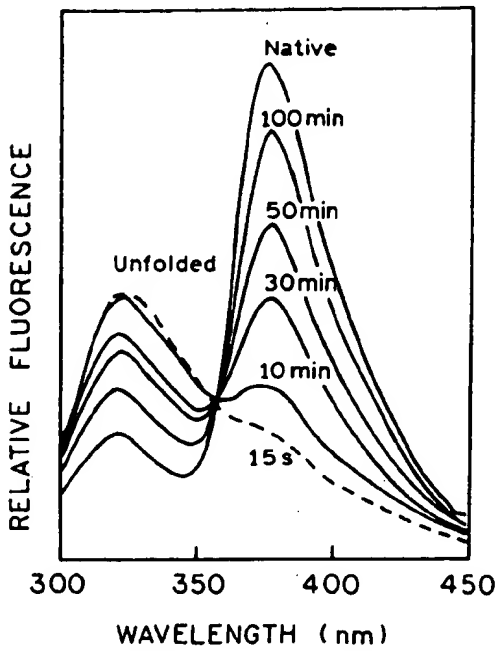

Figure 13.10. Emission spectra of trp-183 in PyP-5′-serine hydroxymethyltransferase during refolding. Excitation at 290 nm. Revised from Ref. 29.

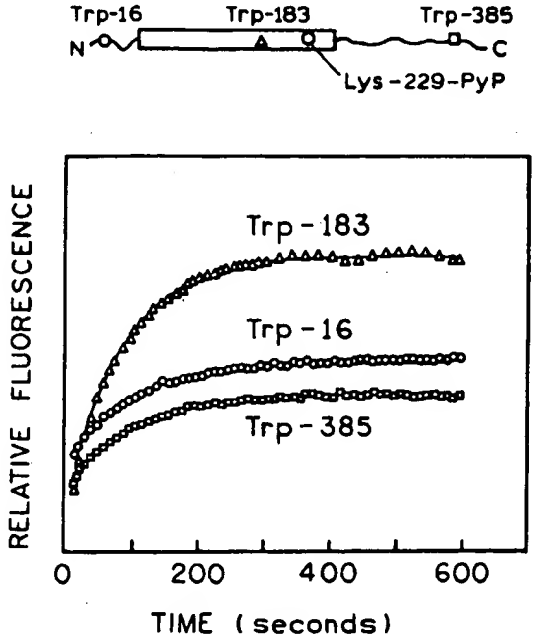

Figure 13.11. Time-dependent intensity of PyP at 380 nm in serine hydroxymethyltransferase during refolding of the single-tryptophan mutants. Excitation at 290 nm. Revised from Ref. 29.

neasured during refolding for each of the mutants (trp-183, trp-16, and trp-385 in Figure 13.11), providing information about the folding pathway. For this protein, the greatest acceptor enhancement is seen for the trp-183 mutant, suggesting that trp-183 is closest to PyP in the folded protein. Less transfer is seen from the other two tryptophan residues. The extent of energy transfer from each tryptophan residue allowed determination of the trp-to-PyP distances. By such experiments, one can determine which region of the protein folds first and thus gain an understanding of the folding pathway. These experiments on protein folding represent an important class of experiments based on protein engineering and site-directed mutagenesis. These techniques of molecular biology make it possible to simplify the spectral signal from multitryptophan proteins to obtain structural information.

3.2.D. Orientation of a Protein-Bound Peptide

In the presence of calcium, calmodulin is known to interact with a number of proteins and peptides. One example is binding of a peptide from myosin light-chain kinase (MLCK) to calmodulin.[30] Such peptides are known to bind in the cleft between the two domains of calmodulin (Figure 13.12). When bound to calmodulin, the MLCK peptide

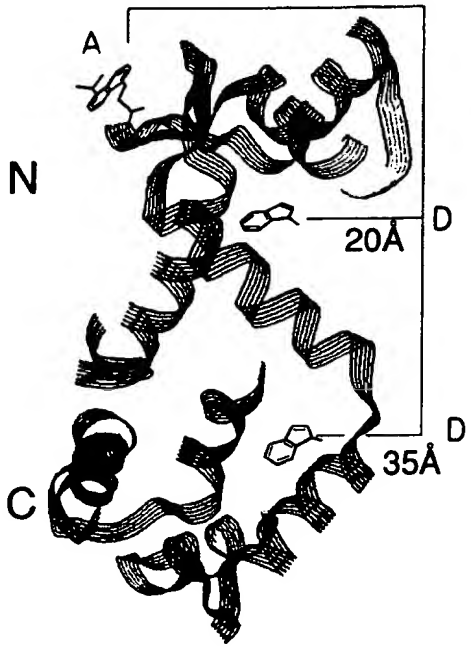

Figure 13.12. Structure of spinach calmodulin. The acceptor is AEDANS on cysteine-26 of calmodulin. The tryptophan donor is on the MLCK peptides shown in Figure 13.13. Revised and reprinted, with permission, from Ref. 30, Copyright © 1992, American Chemical Society.

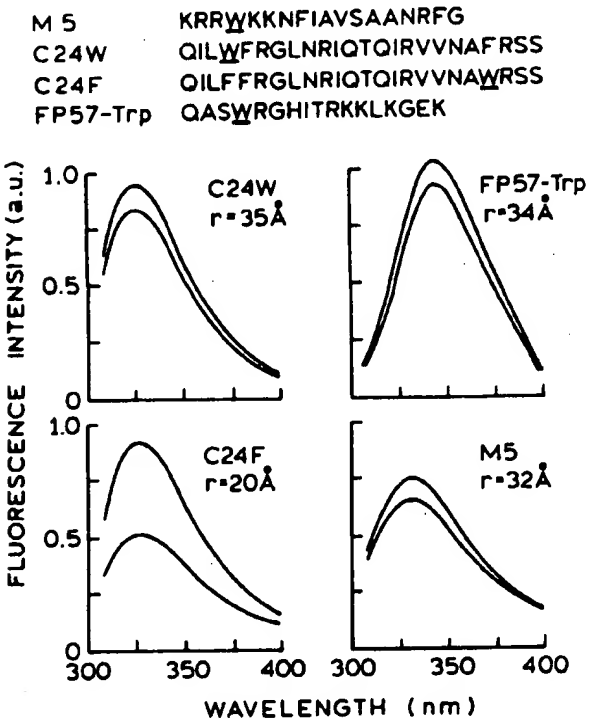

Figure 13.13. Emission spectra of MLCK peptides when free in solution and when bound to AEDANS-calmodulin. The upper and lower spectra in each panel correspond to the peptide emission spectra in the absence and in the presence of AEDANS-calmodulin, respectively. The peptide sequences are shown at the top of the figure, and the calculated distances are shown with the spectra. Excitation was at 295 nm. Revised and reprinted, with permission, from Ref. 30, Copyright © 1992, American Chemical Society.

was known to adopt an α-helical conformation. However, the direction of peptide binding to calmodulin was not known.

Information on the direction of binding was obtained by studying four similar peptides, each of which contained a single tryptophan residue, which served as the donor (Figure 13.13). Calmodulin typically contains only tyrosine residues, so an intrinsic acceptor was not available. This problem was solved by using calmodulin from spinach, which contains a single cysteine residue at position 26. This residue was labeled with 1,5-IAEDANS, which contains a thiol-reactive iodoacetyl group. The Förster distances for trp-to-AEDANS energy transfer ranged from 21 to 24 Å.

Emission spectra of the tryptophan-containing peptides are shown in Figure 13.13. The excitation wavelength was 295 nm to avoid excitation of the tyrosine residues in calmodulin. Upon binding of AEDANS-calmodulin, the tryptophan emission of each peptide was quenched. One of the peptides showed a transfer efficiency of 54%, and the remaining three peptides showed efficiencies ranging from 5 to 16%. These results demonstrated that the N-terminal region of the peptides bound closely to the N-terminal domain of calmodulin and illustrate how structural information can be obtained by comparative studies of analogous structures.

13.3. USE OF RET TO MEASURE MACROMOLECULAR ASSOCIATIONS

Energy transfer is widely useful in biochemistry even apart from its application for the measurement of distances. This is because energy transfer occurs independently of the linker joining the donor and acceptor and depends only on the D–A distance. Hence, any process bringing the donor and acceptor into close proximity will result in energy transfer. This includes biochemical association reactions, as will be illustrated below for protein subunits and DNA oligomers.

13.3.A. Dissociation of the Catalytic and Regulatory Subunits of a Protein Kinase

Cyclic 3′,5′-adenosine monophosphate (cAMP) is an important second messenger in cellular transduction pathways, and it is thus important to develop optical means to detect cAMP. Nucleotides are weakly fluorescent or nonfluorescent, so that it is not practical to use the intrinsic emission of cAMP. One method to detect cAMP is based on the effect of cAMP on the cAMP-dependent protein kinase.[31] The basic idea is to label the protein subunits with donors and acceptors. The presence of cAMP alters the extent of RET, which can be monitored by the donor or acceptor emission.

The cAMP-dependent protein kinase (PK) is composed of four units, two catalytic (C) and two regulatory (R) subunits. These subunits were thought to dissociate in the presence of the substrate cAMP and in the presence of protein kinase inhibitor (PKI). The association of the catalytic (C) and regulatory (R) subunits was examined by covalently labeling the subunits with a fluorescein (Fl-C) and a rhodamine (Rh-R) derivative, respectively.[32] The actual probes used were carboxyfluorescein succinimidyl ester and Texas Red sulfonyl chloride, which is a rhodamine derivative. Absorption and emission spectra are shown in Figure 13.14. The Förster distance for this D–A pair was 51.3 Å and was thus suited for distance measurements between protein subunits. For calculation of R_0, the quantum yield of the donor was taken as 0.5, κ^2 was

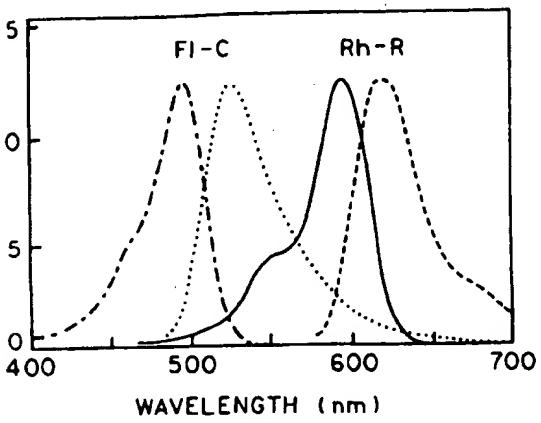

e 13.14. Spectral overlap of the fluorescein-labeled catalytic it (Fl-C) and the Texas Red-labeled regulator subunit (Rh-R) of a -dependent protein kinase. –·–, Absorption spectrum of Fl-C; ···, on spectrum of Fl-C; ———, absorption spectrum of Rh-R; – –, on spectrum of Rh-R. Revised and reprinted, with permission, from 2, Copyright © 1993, American Chemical Society.

ned equal to $\frac{2}{3}$, and the maximum extinction coeffi- of the acceptor was set equal to 85,000 M^{-1} cm^{-1}. on addition of cAMP, the extent of energy transfer ased (Figure 13.15), consistent with a 10-Å increase e D–A distance. This decrease in RET could be preted in terms of a displacement of the donor and otor to more distant regions of the protein (Figure 5). While the extent of RET allows a distance calcula- this is not necessary. The fact that energy transfer still rs in the protein kinase with bound cAMP demon-

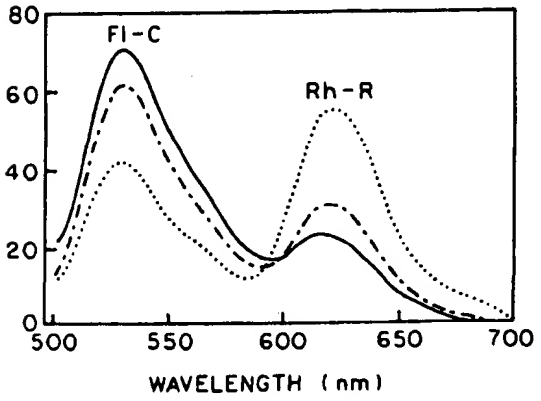

e 13.15. Effect of cAMP and protein kinase inhibitor (PKI) on ission spectrum of a donor- and acceptor-labeled cAMP-dependent n kinase. The emission spectrum of the holoenzyme without cAMP l (···) and the emission spectra recorded following addition of cAMP and PKI (———) are shown. Revised and reprinted, with permis- rom Ref. 32, Copyright © 1993, American Chemical Society.

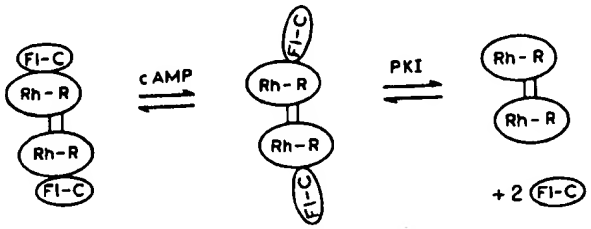

Figure 13.16. Effect of cAMP and protein kinase inhibitor (PKI) on the structure and association of cAMP-dependent protein kinase. The holoenzyme consists of two catalytic and two regulatory subunits. Revised from Refs. 31 and 32.

strates that the subunits are still associated in the presence of cAMP. If the subunits were dissociated by cAMP, energy transfer would be eliminated. This is because for unlinked donors and acceptors, the acceptor concentrations need to be in the millimolar range for Förster transfer to occur (Chapter 15).

The protein kinase was examined further by addition of PKI, which resulted in elimination of energy transfer (Figure 13.15). While one could argue about changes in D–A distance versus protein dissociation as the cause of this effect, the important point from these data is that RET can be used as a proximity sensor. For dilute biochemical solutions, energy transfer between nonassociated species can usually be ignored unless the acceptor concentrations are very high (millimolar). Binding will bring donor and acceptor within the Förster distance, resulting in energy transfer. This example shows how RET can be used to measure the extent of association even without knowledge of the Förster distance. Of course, such data could be used to measure the dissociation constant of cAMP from the protein (Problem 13.6). Calculation of the distance is not needed to calculate the dissociation constant. Use of the donor intensity provides a simple method to monitor the rates and extents of any association reaction.

It is important to remember the possibility of inner filter effects, which can distort the measured intensities of the donors or acceptors.[33] For instance, in the previous example suppose that the fluorescence emission was measured at 550 nm, where the acceptor extinction coefficient is near 33,000 M^{-1} cm^{-1}. To maintain the acceptor absorbance below 0.05, the concentration of the acceptor-labeled protein must be below 1.5μM. If higher acceptor concentrations are used, the intensity values must be corrected for the absorption at the excitation and/or emission wavelength.

13.3.B. RET Calcium Indicators

The dependence of RET on proximity has been used to develop indicators for calcium. One example used a pep-

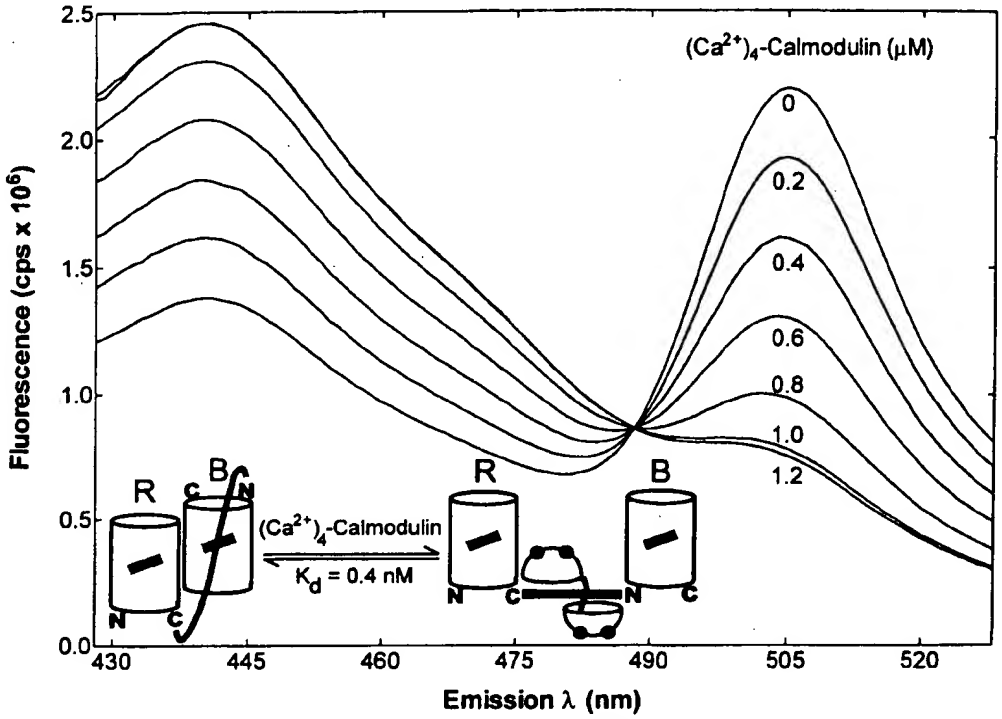

Figure 13.17. An RET calcium indicator composed of calmodulin and two GFP mutants (R and B) linked by the MLCK which binds to calmodulin. From Ref. 34.

tide from MLCK to link two mutants of green fluorescent protein (GFP).[34] By modification of the amino acid sequence of GFP, it is possible to create mutant proteins that emit at shorter or longer wavelengths. Two GFP mutants which would undergo energy transfer, a red (R) and a blue (B) GFP, were selected. These GFPs were placed on opposite ends of the MLCK peptide. In the presence of calcium, calmodulin exposes a hydrophobic surface, which can bind to a number of proteins, including the MLCK peptide. When calmodulin bound the MLCK peptide, the R and B GFPs became more widely separated, and the extent of energy transfer decreased (Figure 13.17). Similar results were obtained for calmodulin covalently linked to the MLCK peptide and the GFPs.[35] An important aspect of this work is that the genes for GFP-labeled proteins can be prepared by molecular biology and expressed in bacteria. This approach bypasses the usual difficulties associated with covalent labeling of specific sites on proteins.

13.3.C. Association Kinetics of DNA Oligomers

The general usefulness of RET in investigations of association reactions is illustrated by studies of donor- and acceptor-labeled DNA oligomers that have a complementary base sequence.[36–38] In such studies, one strand is typically labeled with fluorescein (Fl), and the complementary DNA strand is labeled with rhodamine (Rh) (Figure 13.18). Upon association, the fluorescein donor is quenched.[38] The fluorescence of the donor can be used to measure the rates of association or dissociation of the DNA oligomers (Figure 13.19). In other studies, the extent of RET has been used to detect changes in the melting temperature of DNA oligomers. The melting temperature was found to be sensitive to even a single base pair mismatch.[37]

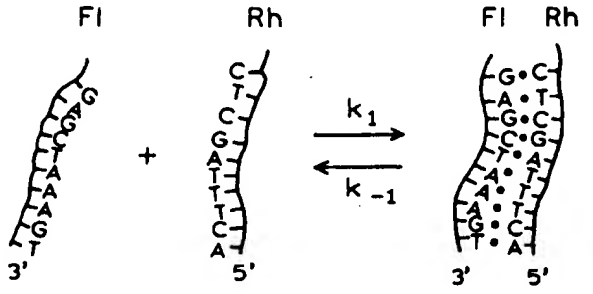

Figure 13.18. DNA association kinetics observed using oligonucleotides labeled with fluorescein (Fl) and rhodamine (Rh). Revised from Ref. 38.

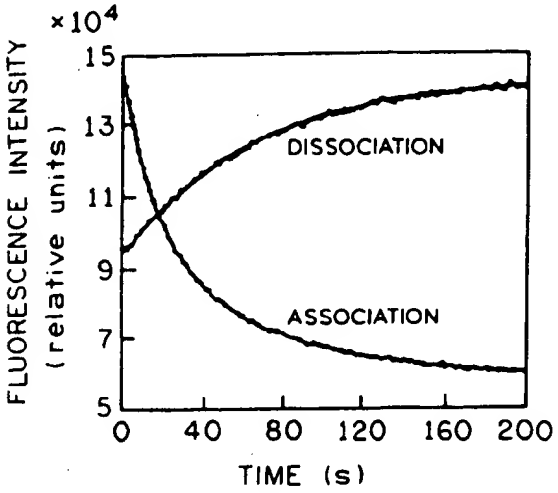

Figure 13.19. Association and dissociation kinetics of complementary donor- and acceptor-labeled oligonucleotides, observed using the donor (fluorescein) emission intensity. Revised and reprinted, with permission, from Ref. 38, Copyright © 1993, American Chemical Society.

RET has also been used to measure the catalytic activity of restriction enzymes, which cleave DNA at specific sites in the sequence. One example of this application is on investigation of the PaeR7 endonuclease.[39] For this restriction enzyme, the recognition site consists of a CTCGAG

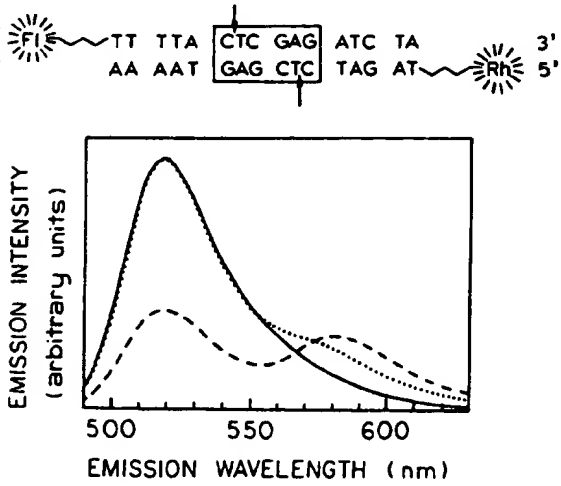

igure 13.20. Principle of the RET endonuclease assay. The emission ectrum of a 16-mer donor strand (—) is quenched upon addition of its mplementary rhodamine-labeled strand (– – –). The fluorescence ectrum taken after addition of PaeR7 endonuclease (· · ·) shows full covery of the fluorescein emission intensity of the donor strand, indiating complete cleavage of the DNA duplex substrate. The peak at 580 n in the emission spectra of duplex samples is due to the rhodamine ceptor fluorescence. Revised from Ref. 39.

sequence. Fluorescein-donor- and rhodamine-acceptor-labeled oligonucleotides served as the substrate (Figure 13.20). Binding of the DNA strands resulted in donor quenching and acceptor enhancement. Digestion with the endonuclease resulted in an increase in donor fluorescence equivalent to that in the donor-only control. When the donors and acceptors are on separate DNA fragments, the solution is too dilute for energy transfer.

The concept used in the endonuclease assay was the elimination of RET by enzymatic breakage of a covalently linked D–A pair. This concept has been applied in a variety of other circumstances,[40] including assay of an HIV-1 endonuclease,[41] which is involved in integrating the HIV into the host DNA. RET has also been used to measure the activity of an HIV protease,[42] proteolytic cleavage of linked derivatives of GFP,[43] and the activity of ribozymes in cleaving RNA[44] and as the basis of a general assay for DNA cleavage.[45]

13.3.D. Energy Transfer Efficiency from Enhanced Acceptor Fluorescence

In a RET experiment the acceptor must absorb light at donor emission wavelengths, but the acceptor does not need to be fluorescent. However, fluorescent acceptors are often used. In these cases, light absorbed by the donor and transferred to the acceptor appears as enhanced acceptor emission. This enhanced acceptor emission can be seen in Figure 13.15 at 620 nm for the Rh-labeled subunits of protein kinase when bound to the Fl-labeled subunits and in Figure 13.20 at 580 nm when the donor and acceptor DNA oligomers are associated. By extrapolating the emission spectrum of the donor, one can see that its emission extends to the acceptor wavelengths. Hence, the intensity measured at the acceptor wavelength typically contains some contribution from the donor.

Use of the acceptor intensities is complicated by the need to account for directly excited acceptor emission, which is almost always present.[11,46] In the case of protein kinase, the acceptor emission without RET (shown as the solid curve in Figure 13.15) is about 40% of the intensity with RET. This occurs because the acceptor absorbs at the excitation wavelength used to excite the donor, resulting in acceptor emission without RET.

Calculation of the transfer efficiency from the enhanced acceptor emission requires careful consideration of all the interrelated intensities. Assuming that the donor does not emit at the acceptor wavelength, the efficiency of transfer is given by

$$E = \frac{\varepsilon_A(\lambda_D^{ex})}{\varepsilon_D(\lambda_D^{ex})}\left[\frac{F_{AD}(\lambda_A^{em})}{F_A(\lambda_A^{em})} - 1\right]\left(\frac{1}{f_D}\right) \qquad [13.25]$$

In this expression, $\varepsilon_A(\lambda_B^{ex})$ and $\varepsilon_D(\lambda_B^{ex})$ are the extinction coefficients (single D–A pairs) or absorbance (multiple acceptors) of the acceptor and the donor at the donor excitation wavelength (λ_B^{ex}), and f_D is the fractional labeling with the donor. The acceptor intensities are measured at an acceptor emission wavelength (λ_A^{em}) in the absence [$F_A(\lambda_A^{em})$] and in the presence [$F_{AD}(\lambda_A^{em})$] of donor. This expression with $f_D = 1.0$ can be readily obtained by noting that $F_A(\lambda_A^{em})$ is proportional to $\varepsilon_A(\lambda_B^{ex})$ and $F_{AD}(\lambda_A^{em})$ is proportional to $\varepsilon_A(\lambda_B^{ex}) + E\varepsilon_D(\lambda_B^{ex})$. The accuracy of the measured E value is typically less than when using the donor emission (Eq. [13.14]).

It is also important to remember that it may be necessary to correct further for the donor emission at λ_A, which is not accounted for in Eq. [13.25]. The possibility of donor emission at λ_A is easily seen from the donor emission spectra in Figures 13.15 and 13.20. The presence of donor emission at the acceptor wavelength, if not corrected for in measuring the acceptor intensities, will result in an apparent transfer efficiency larger than the actual value (see Problem 13.11). Equation [13.25] can also be applied when multiple acceptors are present, that is, in the case of unlinked donor and acceptor pairs (Chapter 15). In this case, $\varepsilon_D(\lambda_D^{ex})$ and $\varepsilon_A(\lambda_D^{ex})$ are replaced by the optical densities of the donor [$OD_D(\lambda_D^{ex})$] and of the acceptor [$OD_A(\lambda_D^{ex})$] at the donor excitation wavelength. The factor $1/f_D$ in Eq. [13.25] is the fractional labeling with the donor. When measuring the acceptor emission, it is important to have complete donor labeling, $f_D = 1.0$.

Occasionally, it is difficult to obtain the transfer efficiency from the sensitized acceptor emission. One difficulty is a precise comparison of the donor-alone and donor–acceptor pair at precisely the same concentration. The need for two samples at the same concentration can be avoided if the donor- and acceptor-labeled sample can be enzymatically digested so as to eliminate energy transfer.[47] Additionally, methods allowing comparison of the donor-alone and donor–acceptor spectra without requiring the concentrations to be the same have been developed. This is accomplished by relying on the shape of the donor emission to subtract its contribution from the emission spectrum of the D–A pair. These methods are best understood by reading the original descriptions.[48,49]

Finally, one should be aware of the possibility that the presence of the acceptor affects the donor fluorescence by a mechanism other than RET. Such effects could occur due to allosteric interactions between the donor and acceptor sites. For example, the acceptor may block diffusion of a quencher to the donor, or it may cause a shift in protein conformation that exposes the donor to solvent. If binding of the acceptor results in quenching of the donor by some other mechanism, then the transfer efficiency determined from the donor will be larger than the true value. In such cases, the transfer efficiency determined from enhanced acceptor emission is thought to be the correct value. The possibility of non-RET donor quenching can be addressed by comparison of the transfer efficiencies observed from donor quenching and acceptor sensitization[50] (see Problem 13.11).

13.4. ENERGY TRANSFER IN MEMBRANES

In the examples of RET described so far, there was a single acceptor attached to each donor molecule. The situation becomes more complex for unlinked donors and acceptors. In this case the bulk concentration of acceptors is important because the acceptor concentration determines the D–A proximity. Also, one needs to consider the presence of more than a single acceptor around each donor. In spite of the complexity, RET has considerable potential for studies of lateral organization in membranes. For example, consider a membrane which contains regions that are in the liquid phase and regions that are in the solid phase. If the donor and acceptor both partition into the same region, one expects the extent of energy transfer to be increased, relative to that expected for a random distribution of donors and acceptors between the phases. Conversely, if donor and acceptor partition into different phases, the extent of energy transfer will decrease relative to a random distribution, an effect which has been observed.[51] Alternatively, consider a membrane-bound protein. If acceptor-labeled lipids cluster around the protein, then the extent of energy transfer will be greater than expected for acceptor randomly dispersed in the membrane. Energy transfer to membrane-localized acceptors can be used to measure the distance of closest approach to a donor site on the protein or the distance from the donor to the membrane surface.

RET in membranes is typically investigated by measuring the transfer efficiency as the membrane acceptor concentration is increased. Quantitative analysis of such data requires knowledge of the extent of energy transfer expected for fluorophores randomly distributed on the surface of a membrane. This is a complex problem which requires one to consider the geometric form of the bilayer (planar or spherical) and transfer between donors and acceptors which are on the same side of the bilayer as well as those on opposite sides. A variety of approaches have been used,[5,52–60] and, in general, numerical simulations and/or computer analyses are necessary. These theories are complex and not easily summarized. The complexity of the problem is illustrated by the fact that an analytical expression for the donor intensity for energy transfer in two

ıensions only appeared in 1964[61] and was extended to ɔw an excluded volume around the donor in 1979.[53] T to multiple acceptors in one, two, and three dimenns is described in more detail in Chapter 15. Several of se results are presented here to illustrate the general m of the expected data.

\ general description of energy transfer on a two-dimenal surface has been given by Fung and Stryer.[5] Assumno homotransfer between the donors, and no diffusion ing the donor excited-state lifetime, the intensity decay he donor is given by

$$I_D(t) = I_D^0 \exp(-t/\tau_D) \exp[-\sigma S(t)] \qquad [13.26]$$

ere

$$S(t) = \int_{r_c}^{\infty} \{1 - \exp[-(t/\tau_D)(R_0/r)^6]\} 2\pi r\, dr \qquad [13.27]$$

hese equations $\exp[-\sigma S(t)]$ describes that portion of the ıor decay due to RET, σ is the surface density of the eptor, and r_c is the distance of closest approach between donor and acceptors. The energy-transfer efficiency be calculated by an equation analogous to Eqs. [13.13] [13.14], except that the intensities or lifetimes are ɔulated from integrals of the donor intensity decay:

$$E = 1 - \frac{1}{\tau_D} \int \frac{I_D(t)}{I_D^0}\, dt \qquad [13.28]$$

quations [13.26]–[13.28] are moderately complex to ve and require use of numerical integration. However, approach is quite general and can be applied to a wide ety of circumstances by using different expressions for that correspond to different geometric conditions. ure 13.21 shows the calculated transfer efficiencies for se in which the donor and acceptors are constrained to lipid–water interface region of a bilayer. Several fea-s of these predicted data are worthy of mention. The ɔiency of transfer increases with R_0 and is independent he concentration of donor. The absence of energy sfer between donors is generally a safe assumption ɔss the donor displays a small Stokes' shift or the donor ɔentration is high, conditions which favor homotrans-Only small amounts of acceptor, 0.4 mol %, can result asily measured quenching. For example, with $R_0 = 40$ ıe transfer efficiency is near 50% for just 0.8 mol % ɔptor, or one acceptor per 125 phospholipid molecules. ne may readily visualize how energy quenching data ıd be used to determine whether the distributions of or and acceptor are random. Using the calculated value o, one compares the measured extent of donor quenching with the observed efficiency. If the measured quenching efficiency exceeds the calculated value, then a preferential association of donors and acceptors within the membrane is indicated.[62] Less quenching would be observed if the donor and acceptor are localized in different regions of the membrane or if the distance of closest approach is restricted due to steric factors. We note that these calculated values shown in Figure 13.21 are strictly true only for transfer between immobilized donor and acceptor on one side of a planar bilayer. However, this simple model is claimed to be a good approximation for a spherical bilayer.[5] For smaller values of R_0, transfer across the bilayer is not significant.

It is also instructive to examine the time-resolved decays of the donor in the presence of acceptor (Figure 13.22). In the presence of acceptor, the donor decays become significantly nonexponential, especially at higher acceptor concentrations. The origin of this nonexponential decay is the time-dependent distribution of acceptors around the excited donors. At short times following excitation, there exist more donors with nearby acceptors. The donors with nearby acceptors decay more rapidly because of the dis-

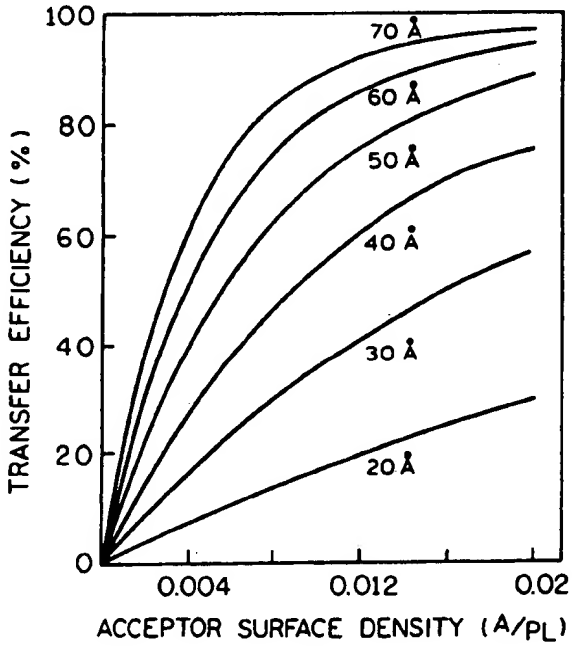

Figure 13.21. Calculated efficiencies of energy transfer for donor–acceptor pairs localized in a membrane. The distances labeled on the curves are the R_0 values for energy transfer, and A/PL is the acceptor-to-phospholipid molar ratio. The area per phospholipid was assumed to be 70 $Å^2$, so the distance of closest approach was 8.4 Å. Revised from Ref. 5.

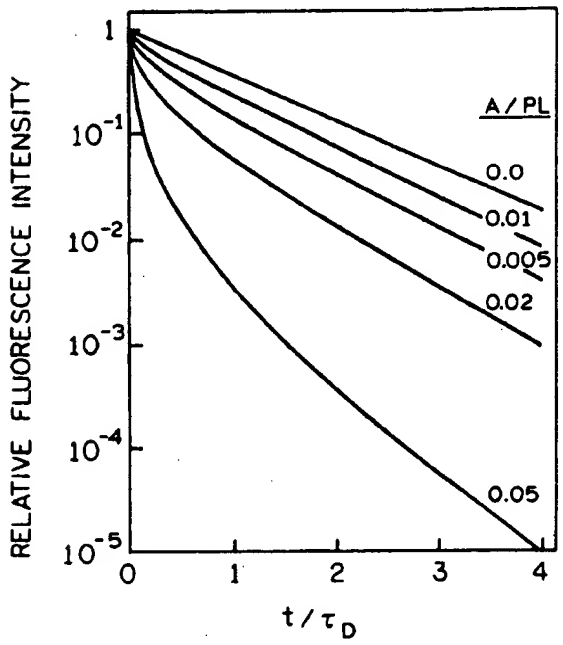

Figure 13.22. Calculated time-resolved decays of donor fluorescence for membrane-bound donors and acceptors. For these calculations R_0 = 40 Å. The values labeled on the curves are the acceptor-to-phospholipid molar ratios (A/PL). Revised from Ref. 5.

tance dependence of energy transfer. At later times, the donors with nearby acceptors have decayed, and the emission results preferentially from donors without nearby acceptors. The decay time of these donors is longer, owing to a slower rate of energy transfer to more distant acceptors.

There is considerable information in these time-resolved decays, and methods to recover this information are described in Chapter 15. In the more general case, the distance between donor and acceptor can vary both as a result of a range of distances and by diffusion. Both factors affect the rates of energy transfer and must be considered in any such analysis.

13.4.A. Lipid Distributions around Gramicidin

Gramicidin is a linear polypeptide antibiotic containing D-and L-amino acids and four tryptophan residues. Its mode of action involves increasing the permeability of membranes to cations and protons. In membranes, this peptide forms a dimer (Figure 13.23)[63] that contains a 4-Å diameter aqueous channel which allows diffusion of cations. The nonpolar amino acids are present on the outside of the helix and are thus expected to be exposed to the acyl side-chain region of the membrane. Hence, gramicidin provides an ideal model with which to examine energy transfer from a membrane-bound protein to membrane-bound acceptors.

It was of interest to determine if membrane-bound gramicidin was surrounded by specific types of phospholipids. This question was addressed by measurement of the transfer efficiencies from the tryptophan donor to dansyl-labeled phosphatidylcholine (PC), 1-acyl-2-[11-[*N*-[5-(dimethylamino)naphthalene-1-sulfonyl]amino]undecanoyl]phosphatidylcholine. The lipid vesicles were composed of PC and phosphatidic acid (PA).[64] Emission spectra of gramicidin bound to PC–PA membranes are

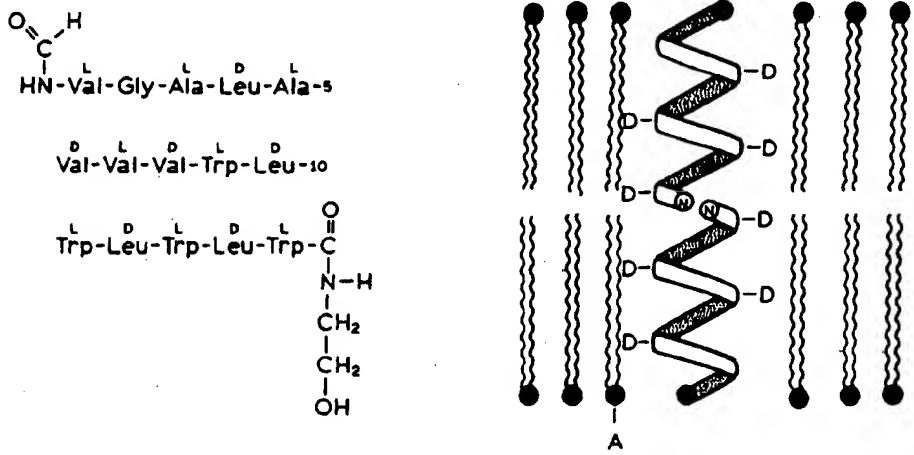

Figure 13.23. Amino acid sequence (*left*) and structure of the membrane-bound dimer (*right*) of gramicidin A. In the amino acid sequence, D and L refer to the optical isomer of the amino acid. Revised from Ref. 63.

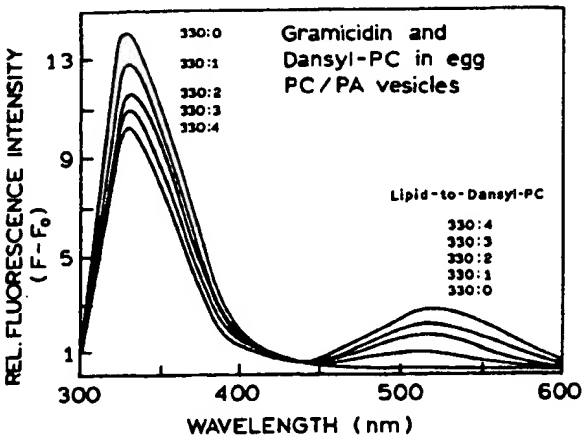

Figure 13.24. Dansyl-PC is 1-acyl-2-[11-[*N*-[5-(dimethylamino)naphthalene-1-sulfonyl]amino]undecanoyl]phosphatidylcholine. Emission spectra of gramicidin and dansyl-PC in vesicles composed of egg PC and egg PA. λ_{ex} = 282 nm. The lipid-to-dansyl-PC ratios are shown on the figure. Revised and reprinted, with permission, from Ref. 64, Copyright © 1988, American Chemical Society.

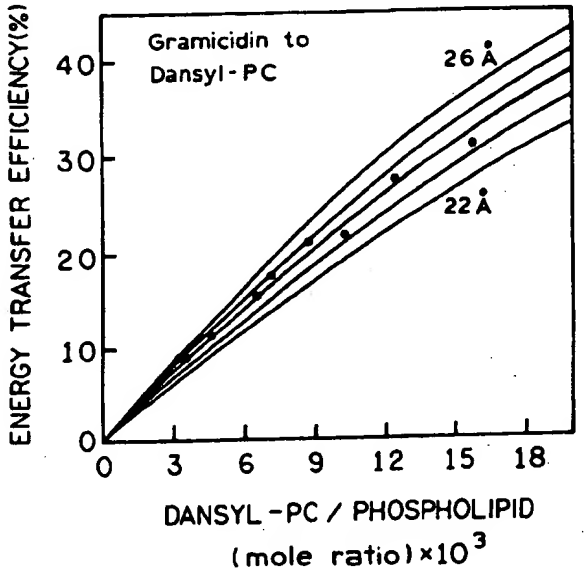

Figure 13.25. Efficiency of energy transfer from gramicidin to dansyl-PC as a function of dansyl-PC/phospholipid ratio. The experimental points (•) were calculated from the tryptophan quenching data, and the solid curves were calculated for a random array of donors and acceptors in two dimensions with R_0 = 22, 23, 24, 25, and 26 Å. A value of R_0 = 24 ± 1 Å gave the best fit to the experimental data. Revised and reprinted with permission from Ref. 64, Copyright © 1988, American Chemical Society.

shown in Figure 13.24. The tryptophan emission is progressively quenched as the dansyl-PC acceptor concentration is increased. The fact that the gramicidin emission is quenched by RET, rather than a collisional process, is supported by the enhanced emission of the dansyl-PC at 520 nm.

The decreasing intensities of the gramicidin emission can be used to determine the tryptophan-to-dansyl-PC transfer efficiencies, as shown in Figure 13.25. The transfer efficiencies are compared with the calculated efficiencies for a random acceptor distribution in two dimensions. These efficiencies were calculated for various values of R_0 using Eqs. [13.26] and [13.28]. The data match the curve calculated for the known R_0 of 24 Å, demonstrating that the distribution of the dansyl-PC acceptors around gramicidin is random. If a particular lipid (PC, PE, or PA) was localized around gramicidin, then RET to the dansyl analog would exceed the calculated values.

13.4.B. Distance of Closest Approach in Membranes

In addition to determining the randomness of lipid distributions, it is also possible to determine the distance of closest approach (r_c) between a membrane-bound protein and an acceptor-labeled lipid. One example is the use of energy transfer to study skeletal protein 4.1.[65] In this case the protein was labeled with IAEDANS, a sulfhydryl-selective dansyl derivative. The acceptor was 3,3′-ditetradecyloxacarbocyanine perchlorate [di-O-C_{14}-(3)], resulting in an R_0 value of 57 Å. Emission spectra are shown in the upper panel of Figure 13.26 for the donor-labeled, acceptor-labeled, and doubly labeled samples as well as the unlabeled sample. The latter spectrum illustrates the need for recording the emission spectra of control samples that do not contain the fluorophores. Depending on the wavelength, the background signal can vary from 20 to nearly 100% of the measured intensity.

In the presence of increasing amounts of acceptor-labeled lipid, the donor-labeled protein is quenched (Figure 13.26, bottom). The fact that the shape of the donor emission spectrum is changing indicates that part of the donor quenching is due to inner filtering by the acceptor absorbance. These data were used to determine the transfer efficiencies to the lipid-bound cyanine dye (Figure 13.27). In this case, the predicted transfer efficiencies were obtained from a simple numerical table[54] which provides a biexponential approximation for various values of r_c/R_0. Use of this table circumvents the need for numerical integration of Eqs. [13.26] and [13.28].

The transfer efficiencies are compared with the calculated curves for various distances of closest approach. As the distance of closest approach becomes larger, the calculated transfer efficiency decreases. The data indicate that the acceptor cannot be closer than 77 Å from the donor-la-

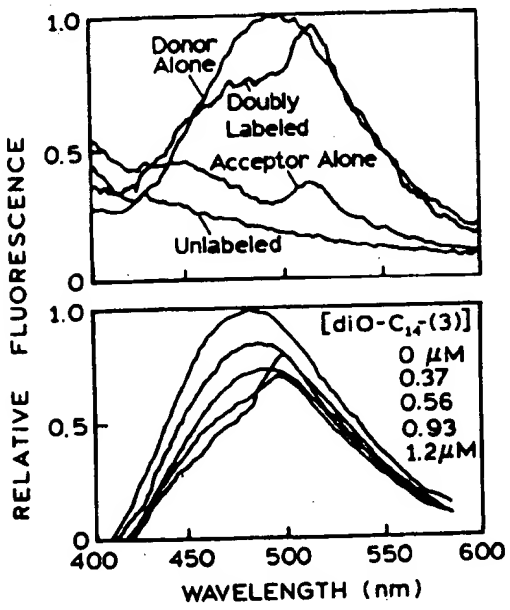

Figure 13.26. *Top:* Emission spectra of skeletal protein 4.1 and of donor-labeled acceptor-labeled, and doubly labeled samples. The donor is IAEDANS and the acceptor is diO-C_{14}-(3). *Bottom:* Emission spectra of IAEDANS-labeled skeletal protein 4.1 in the presence of lipid-bound diO-C_{14}-(3) acceptor. The lipid concentration was 55.4μM, and the acceptor concentrations are shown on the figure. Excitation was at 334 nm. Revised from Ref. 65.

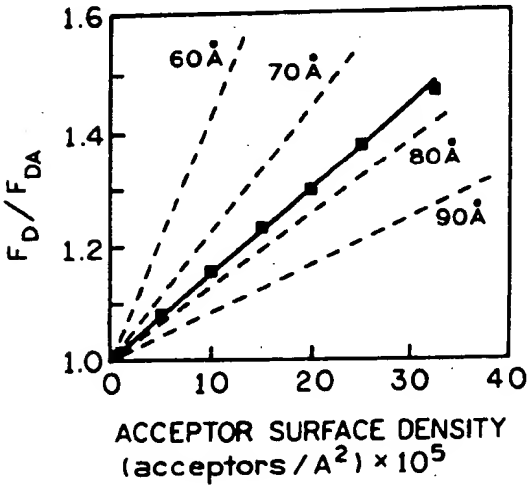

Figure 13.27. RET efficiency from IAEDANS-labeled skeletal protein 4.1 to a lipid-bound cyanine dye. The dashed lines are the predicted transfer efficiencies for various distances of closest approach, calculated according to Ref. 54. Revised from Ref. 65.

beled site and that the donor-labeled site in skeletal protein 4.1 is located deep in the protein. These results suggested that other domains in the protein prevent closer approach of the acceptor.[65] There have been many other reports on energy transfer in membranes, only a few of which can be cited here.[66–69]

13.4.C. Membrane Fusion and Lipid Exchange

Energy transfer has been widely used to study fusion and/or aggregation of membranes. These experiments are shown schematically in Figure 13.28. Suppose that a vesicle contains donor and a surface density of acceptor adequate to quench the donor. As seen from Figure 13.21, the acceptor density does not need to be large. Any process which dilutes the donor and acceptors from the initially labeled vesicles will result in less energy transfer and increased donor emission. For example, if the D–A-labeled residues fuse with an unlabeled vesicle, the acceptor becomes more dilute and the donor intensity increases (Figure 13.28, top). Alternatively, the donor may display a modest water solubility adequate to allow exchange between vesicles (Figure 13.28, left). Then some of the donors will migrate to the acceptor-free vesicles, and again the donor fluorescence will increase. It is also possible to trap a water-soluble fluorophore–quencher pair inside the vesicles. Upon fusion, the quencher can be diluted and/or released. A wide variety of different procedures have been proposed,[70–74] but most rely on these simple proximity considerations.

13.5. ENERGY TRANSFER IN SOLUTION

Energy transfer also occurs for donors and acceptors randomly distributed in three-dimensional solutions. In this case the theory is relatively simple. Following δ-function excitation, the intensity decay of the donor is given by[75–77]

$$I_D(t) = I_D^0 \exp\left[\frac{-t}{\tau_D} - 2\gamma\left(\frac{t}{\tau_D}\right)^{1/2}\right] \qquad [13.29]$$

with $\gamma = A/A_0$, where A is the acceptor concentration. If R_0 is expressed in centimeters, the value of A_0 in moles per liter is given by

$$A_0 = \frac{3000}{2\pi^{3/2} N R_0^3} \qquad [13.30]$$

The relative steady-state quantum yield of the donor is given by

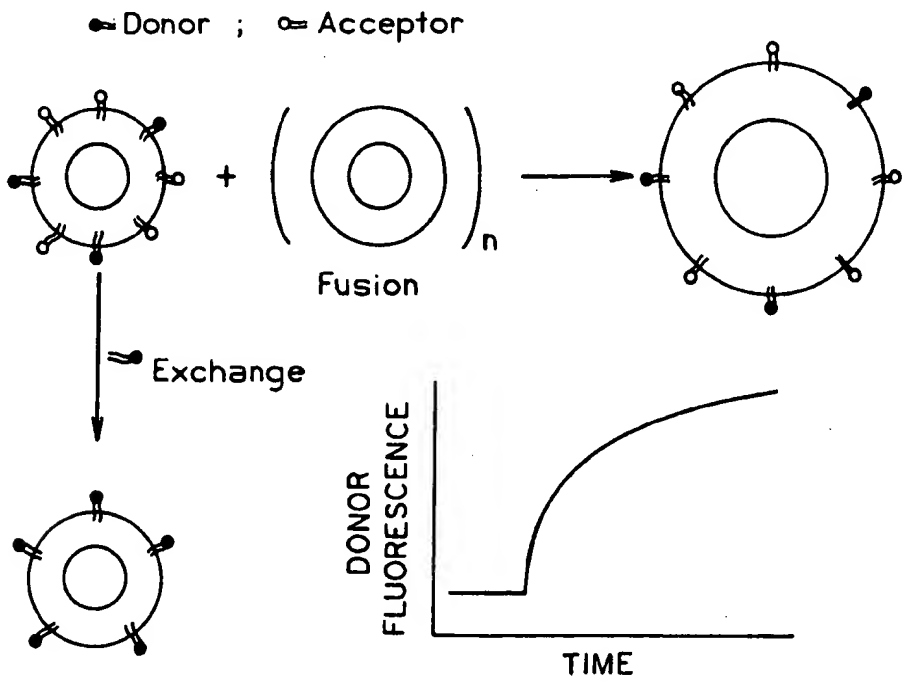

Figure 13.28. Lipid exchange and membrane fusion assays based on energy transfer. Exchange of the donor or acceptor to unlabeled vesicles or fusion of D–A-labeled vesicles with unlabeled vesicles results in dilution of the D–A pairs and increased donor intensities.

$$\frac{F_{DA}}{F_D} = 1 - \sqrt{\pi}\,\gamma \exp(\gamma^2)[1 - \mathrm{erf}(\gamma)] \qquad [13.31]$$

where

$$\mathrm{erf}(\gamma) = \frac{2}{\sqrt{\pi}} \int_0^{\gamma} \exp(-x^2)\,dx \qquad [13.32]$$

These expressions are valid for immobile donors and acceptors for which the orientation factor is randomized by rotational diffusion ($\kappa^2 = \frac{2}{3}$). For randomly distributed acceptors,[3] where rotation is much slower than the donor decay, $\kappa^2 = 0.476$. Still more complex expressions are necessary if the donor and acceptor diffuse during the lifetime of the excited state (Chapters 14 and 15). The complex decay of donor fluorescence reflects the time-dependent population of D–A pairs. Those donors with nearby acceptors decay more rapidly, and donors more distant from acceptors decay more slowly.

The term A_0 is called the critical concentration and represents the acceptor concentration that results in 76% energy transfer. This concentration, in moles per liter (M), can be calculated from Eq. [13.30] or from a simplified expression,[12]

$$A_0 = 447/R_0^3 \qquad [13.33]$$

where R_0 is in units of angstroms. This reveals an important feature of energy transfer between unlinked donors and acceptors, which is that the acceptor concentrations need to be rather high for RET between unlinked donor and acceptors. For instance, if $R_0 = 25$ Å, then $A_0 = 0.029M = 29mM$. This is why we usually ignore energy transfer between donors and acceptors in different linked D–A pairs. However, it is important to consider inner filter effects when one is comparing intensity values. The high acceptor concentrations needed for RET in solution also make such measurements difficult. The high acceptor concentrations result in high optical densities, requiring front-face observation and careful correction for inner filter effects.

13.5.A. Diffusion-Enhanced Energy Transfer

To this point, we have not considered the effects of diffusion on the extent of energy transfer. This is a complex topic, and typically numerical methods are required for simulations and analysis of these effects. However, one simple case is that in which the donor decay times are very long so that diffusive motions of the donors result in their sampling of the entire available space. This is called the rapid-diffusion limit.[78] With fluorophores displaying nanosecond decay times, this limit is not obtainable. However, lanthanides are known to display much longer decay

times—near 0.6–2.5 ms for terbium and europium,[79,80] depending upon the ligands. In relatively fluid solution, the long donor decay times allow the excited donor molecule to diffuse through all available space. The rate of transfer then becomes limited by the distance of closest approach between donors and acceptors. Suppose that an acceptor is buried in a protein or a membrane. One can determine the depth of the acceptor from the extent of energy transfer to the acceptor from terbium or europium chelates in the aqueous phase. Another important feature of energy transfer in the rapid-diffusion limit is that it occurs at much lower acceptor concentrations.[78] For a homogeneous three-dimensional solution, energy transfer is 50% efficient at acceptor concentrations near 1 μM, which is 1000-fold lower than for energy transfer without diffusion.[12] This topic is described in detail in Section 15.4.

13.6. REPRESENTATIVE R_0 VALUES

It is often convenient to have an estimate of an R_0 value prior to performing the complex calculation of the overlap integral or labeling of the macromolecule. Unfortunately, there is no general reference for the Förster distances. A larger number of R_0 values are summarized in a book by Berlman,[81] but most of the listed fluorophores are not used in biochemistry. A large number of Förster distances have been summarized in a recent review,[12] and useful examples with spectra are given in a review by Fairclough and Cantor.[82] Some of these R_0 values are summarized in Table 13.3 for a variety of D–A pairs and in Table 13.4 for tryptophan D–A pairs. In the case of lanthanides in environments where the quantum yield is near unity, and for a multichromophore acceptor, R_0 values as large as 90 Å have been calculated.[82] This is the largest Förster distance reported to this time.

Table 13.3. Representative Förster Distances for Various Donor–Acceptor Pairs[a,b]

Donor	Acceptor	R_0 (Å)	Reference
Naphthalene	Dansyl	22	12
Dansyl	FITC	33–41	82
Dansyl	ODR	43	12
ε-A	NBD	38	12
IAF	TMR	37–50	12
Pyrene	Coumarin	39	12
FITC	TMR	49–54	12
IAEDANS	FITC	49	12
IAEDANS	IAF	46–56	12
IAF	EIA	46	12
BODIPY	BODIPY	57	21
BPE	Cy5	72	12
Terbium	Rhodamine	65	23
Europium	Cy5	70	79
Europium	APC	90	83

[a]Values are from Refs. 12, 20, 23, 79, 82, and 83, which should be consulted for further details.

[b]Abbreviations: Dansyl, 5-dimethylamino-1-naphthalenesulfonic acid; ε-A, 1-N^6-ethenoadenosine; IAF, 5-(iodoacetamido)fluorescein; FITC, fluorescein 5-isothiocyanate; IAEDANS, 5-(((2-iodoacetyl)amino)ethyl)amino) naphthalene-1-sulfonic acid; CF, carboxyfluorescein, succinimidyl ester; BODIPY, 4,4-difluoro-4-bora-3a,4a-diaza-s-indacene; BPE, B-phycoerythrin; ODR, octadecylrhodamine; NBD, 7-nitrobenz-2-oxa-1,3-diazol-4-yl; TMR, tetramethylrhodamine; EIA, 5-(iodoacetetamido)eosin; TR, Texas Red; Cy5, carboxymethylindocyanine-*N*-hydroxysuccinimidyl ester; APC, allophycocyanin.

Table 13.4. Förster Distances for Tryptophan–Acceptor Pairs[a]

Acceptor[b]	R_0 (Å)
Nitrobenzoyl	16
Dansyl	21–24
IAEDANS	22
Anthroyloxy	24
TNB	24
Anthroyl	25
Tyr-NO_2	26
Pyrene	28
Heme	29
NBS	30
DNBS	33
DPH	40

[a]From Ref. 12.

[b]Abbreviations: Dansyl, 5-dimethylamino-1-naphthalenesulfonic acid; IAEDANS, 5-(((2-iodoacetyl)amino)ethyl)amino)naphthalene-1-sulfonic acid; TNB, trinitrophenyl; NBS, nitrobenzenesulfenyl; DNBS, dinitrobenzenesulfonyl; DPH, 1,6-diphenyl-1,3,5-hexatriene.

REFERENCES

1. Förster, Th., 1948, Intermolecular energy migration and fluorescence, *Ann. Phys.* 2:55–75. Translated by R. S. Knox, Department of Physics and Astronomy, University of Rochester, Rochester, NY 14627.
2. Stryer, L., 1978, Fluorescence energy transfer as a spectroscopic ruler, *Annu. Rev. Biochem.* 47:819–846.
3. Steinberg, I. Z., 1971, Long-range nonradiative transfer of electronic excitation energy in proteins and polypeptides, *Annu. Rev. Biochem.* 40:83–114.
4. Clegg, R. M., 1996, Fluorescence resonance energy transfer, in *Fluorescence Imaging Spectroscopy and Microscopy*, X. F. Wang and B. Herman (eds.), John Wiley & Sons, New York, pp. 179–252.
5. Fung, B. K. K., and Stryer, L., 1978, Surface density determination in membranes by fluorescence energy transfer, *Biochemistry* 17:5241–5248.

6. Weller, A., 1974, Theodor Förster, *Ber. Bunsen-Ges. Phys. Chem.* **78**:969–971.
7. Gordon, M., and Ware, W. R. (eds.), 1975, *The Exciplex*, Academic Press, New York.
8. Dale, R. E., Eisinger, J., and Blumberg, W. E., 1979, The orientational freedom of molecular probes. The orientation factor in intramolecular energy transfer, *Biophys. J.* **26**:161–194. Erratum **30**:365 (1980).
9. Dale, R. E., and Eisinger, J., 1975, Polarized excitation energy transfer, in *Biochemical Fluorescence, Concepts*, Vol. 1. R. F. Chen and H. Edelhoch (eds.), Marcel Dekker, New York, pp. 115–284.
10. Dale, R. E., and Eisinger, J., 1974, Intramolecular distances determined by energy transfer. Dependence on orientational freedom of donor and acceptor, *Biopolymers* **13**:1573–1605.
11. Cheung, H. C., 1991, Resonance energy transfer, in *Topics in Fluorescence Spectroscopy, Vol. 2, Principles*, J. R. Lakowicz (ed.), Plenum Press, New York, pp. 127–176.
12. Wu, P., and Brand, L., 1994, Review—resonance energy transfer: Methods and applications, *Anal. Biochem.* **218**:1–13.
13. Dos Remedios, C. G., and Moens, P. D. J., 1995, Fluorescence resonance energy transfer spectroscopy is a reliable "ruler" for measuring structural changes in proteins, *J. Struct. Biol.* **115**:175–185.
14. Haas, E., Katchalski-Katzir, E., and Steinberg, I. Z., 1978, Effect of the orientation of donor and acceptor on the probability of energy transfer involving electronic transitions of mixed polarizations, *Biochemistry* **17**:5064–5070.
15. Latt, S. A., Cheung, H. T., and Blout, E. R., 1965, Energy transfer. A system with relatively fixed donor–acceptor separation, *J. Am. Chem. Soc.* **877**:996–1003.
16. Stryer, L., and Haugland, R. P., 1967, Energy transfer: A spectroscopic ruler, *Proc. Natl. Acad. Sci. U.S.A.* **58**:719–726.
17. Gabor, G., 1968, Radiationless energy transfer through a polypeptide chain, *Biopolymers* **6**:809–816.
18. Haugland, R. P., Yguerabide, J., and Stryer, L., 1969, Dependence of the kinetics of singlet–singlet energy transfer on spectral overlap, *Proc. Natl. Acad. Sci. U.S.A.* **63**:23–30.
19. Horrocks, W. DeW., Holmquist, B., and Vallee, B. L., 1975, Energy transfer between terbium(III) and cobalt(II) in thermolysin: A new class of metal–metal distance probes, *Proc. Natl. Acad. Sci. U.S.A.* **72**:4764–4768.
20. Johnson, I. D., Kang, H. C., and Haugland, R. P., 1991, Fluorescent membrane probes incorporating dipyrromethemeneboron difluoride fluorophores, *Anal. Biochem.* **198**:228–237.
21. Hemmila, I. A. (ed.), 1991, *Applications of Fluorescence in Immunoassays*, John Wiley & Sons, New York. (See p. 113.)
22. Kawski, A., 1983, Excitation energy transfer and its manifestation in isotropic media, *Photochem. Photobiol.* **38**:487–504.
23. Selvin, P. R., 1995, Fluorescence resonance energy transfer, *Methods Enzymol.* **246**:300–334.
24. Lakowicz, J. R., Gryczynski, I., Wiczk, W., Laczko, G., Prendergast, F. C., and Johnson, M. L., 1990, Conformational distributions of melittin in water/methanol mixtures from frequency-domain measurements of nonradiative energy transfer, *Biophys. Chem.* **36**:99–115.
25. Faucon, J. F., Dufourca, J., and Lurson, C., 1979, The self-association of melittin and its binding to lipids, *FEBS Lett.* **102**:187–190.
26. Goto, Y., and Hagihara, Y., 1992, Mechanism of the conformational transition of melittin, *Biochemistry* **31**:732–738.
27. Bazzo, R., Tappin, M. J., Pastore, A., Harvey, T. S., Carver, J. A., and Campbell, I. D., 1988, The structure of melittin: A ^{1}H-NMR study in methanol, *Eur. J. Biochem.* **173**:139–146.
28. Lakowicz, J. R., Gryczynski, I., Cheung, H. C., Wang, C.-K., Johnson, M. L., and Joshi, N., 1988, Distance distributions in proteins recovered by using frequency-domain fluorometry. Applications to troponin I and its complex with troponin C, *Biochemistry* **27**:9149–9160.
29. Cai, K., and Schircht, V., 1996, Structural studies on folding intermediates of serine hydroxymethyltransferase using fluorescence resonance energy transfer, *J. Biol. Chem.* **271**:27311–27320.
30. Chapman, E. R., Alexander, K., Vorherr, T., Carafoli, E., and Storm, D. R., 1992, Fluorescence energy transfer analysis of calmodulin–peptide complexes, *Biochemistry* **31**:12819–12825.
31. Adams, S. R., Bacskai, B. J., Taylor, S. S., and Tsien, R. Y., 1993, Optical probes for cyclic AMP, in *Fluorescent and Luminescent Probes for Biological Activity*, W. T. Mason (ed.), Academic Press, New York, pp. 133–149.
32. Johnson, D. A., Leathers, V. L., Martinez, A.-M., Walsh, D. A., and Fletcher, W. H., 1993, Biomedical example: Use of FRET to measure subunit associations of the regulation (R) and catalytic (C) subunits of a protein kinase, *Biochemistry* **32**:6402–6410.
33. Guptasarma, P., and Raman, B., 1995, Use of tandem cuvettes to determine whether radiative (trivial) energy transfer can contaminate steady-state measurements of fluorescence resonance energy transfer, *Anal. Biochem.* **230**:187–191.
34. Romoser, V. A., Hinkle, P. M., and Persechini, A., 1997, Detection in living cells of Ca^{2+}-dependent changes in the fluorescence emission of an indicator composed of two green fluorescent protein variants linked by a calmodulin-binding sequence, *J. Biol. Chem.* **272**:13270–13274.
35. Miyawaki, A., Llopis, J., Heim, R., McCaffery, J. M., Adams, J. A., Ikura, M., and Tsien, R. Y., 1997, Fluorescent indicators for Ca^{2+} based on green fluorescent proteins and calmodulin, *Nature* **388**:882–887.
36. Cardullo, R. A., Agrawal, S., Flores, C., Zamecbnik, P. C., and Wolf, D. E., 1988, Detection of nucleic acid hybridization by nonradiative fluorescence resonance energy transfer, *Proc. Natl. Acad. Sci. U.S.A.* **85**:8790–8794.
37. Parkhurst, K. M., and Parkhurst, L. J., 1996, Detection of point mutations in DNA by fluorescence energy transfer, *J. Biomed. Opt.* **1**:435–441.
38. Morrison, L. E., and Stols, L. M., 1993, Use of FRET to measure association of DNA oligomers, *Biochemistry* **32**:3095–3104.
39. Ghosh, S. S., Eis, P. S., Blumeyer, K., Fearon, K., and Millar, D. P., 1994, Real time kinetics of restriction endonuclease cleavage monitored by fluorescence resonance energy transfer, *Nucleic Acids Res.* **22**:3155–3159.
40. Le Bonniec, B. F., Myles, T., Johnson, T., Knight, C. G., Tapparelli, C., and Stones, S. R., 1996, Characterization of the P'_2 and P'_3 specificities of thrombin using fluorescence-quenched substrates and mapping of the subsites by mutagenesis, *Biochemistry* **35**:7114–7122.
41. Lee, S. P., Censullo, M. L., Kim, H. G., Knutson, J. R., and Han, M. K., 1995, Characterization of endonucleolytic activity of HIV-1 integrase using a fluorogenic substrate, *Anal. Biochem.* **227**:295–301.
42. Mayayoshi, E. D., Wang, G. T., Krafft, G. A., and Erickson, J., 1990, Novel fluorogenic substrates for assaying retroviral proteases by resonance energy transfer, *Science* **247**:954–958.
43. Mitra, R. D., Silva, C. M., and Youvan, D. C., 1996, Fluorescence resonance energy transfer between blue-emitting and red-shifted excitation derivatives of the green fluorescent protein, *Gene* **173**:13–17.

44. Perkins, T. A., Wolf, D. E., and Goodchild, J., 1996, Fluorescence resonance energy transfer analysis of ribozyme kinetics reveals the mode of action of a facilitator oligonucleotide, *Biochemistry* 35:16370–16377.
45. Lee, P., and Han, M. K., 1997, Fluorescence assays for DNA cleavage, *Methods Enzymol.* 278:343–361.
46. Bilderback, T., Fulmer, T., Mantulin, W. W., and Glaser, M., 1996, Substrate binding causes movement in the ATP binding domain of *Escherichia coli* adenylate kinase, *Biochemistry* 35:6100–6106.
47. Epe, B., Steinhauser, K. G., and Woolley, P., 1983, Theory of measurement of Förster-type energy transfer in macromolecules, *Proc. Natl. Acad. Sci. U.S.A.* 80:2579–2583.
48. Clegg, R. M., 1992, Fluorescence resonance energy transfer and nucleic acids, *Methods Enzymol.* 211:353–388.
49. Clegg, R. M., Murchie, A. I. H., and Lilley, D. M., 1994, The solution structure of the four-way DNA junction at low-salt conditions: A fluorescence resonance energy transfer analysis, *Biophys. J.* 66:99–109.
50. Berman, H. A., Yguerabide, J., and Taylor, P., 1980, Fluorescence energy transfer on acetylcholinesterase: Spatial relationships between peripheral site and active center, *Biochemistry* 19:2226–2235.
51. Pedersen, S., Jorgensen, K., Baekmark, T. R., and Mouritsen, O. G., 1996, Indirect evidence for lipid-domain formation in the transition region of phospholipid bilayers by two-probe fluorescence energy transfer, *Biophys. J.* 71:554–560.
52. Estep, T. N., and Thomson, T. E., 1979, Energy transfer in lipid bilayers, *Biophys. J.* 26:195–207.
53. Wolber, P. K., and Hudson, B. S., 1979, An analytical solution to the Förster energy transfer problem in two dimensions, *Biophys. J.* 28:197–210.
54. Dewey, T. G., and Hammes, G. G., 1980, Calculation of fluorescence resonance energy transfer on surfaces, *Biophys. J.* 32:1023–1035.
55. Shaklai, N., Yguerabide, J., and Ranney, H. M., 1977, Interaction of hemoglobin with red blood cell membranes as shown by a fluorescent chromophore, *Biochemistry* 16:5585–5592.
56. Snyder, B., and Freire, E., 1982, Fluorescence energy transfer in two dimensions, *Biophys. J.* 40:137–148.
57. Bastiaens, P., de Beus, A., Lacker, M., Somerharju, P., Vauhkonen, M., and Eisinger, J., 1990, Resonance energy transfer from a cylindrical distribution of donors to a plane of acceptors, *Biophys. J.* 58:665–675.
58. Yguerabide, J., 1994, Theory for establishing proximity relations in biological membranes by excitation energy transfer measurements, *Biophys. J.* 66:683–693.
59. Dewey, T. G., 1991, Fluorescence energy transfer in membrane biochemistry, in *Biophysical and Biochemical Aspects of Fluorescence Spectroscopy*, T. G. Dewey (ed.), Plenum Press, New York, pp. 197–230.
60. Dobretsov, G. E., Kurek, N. K., Machov, V. N., Syrejshchikova, T. I., and Yakimenko, M. N., 1989, Determination of fluorescent probes localization in membranes by nonradiative energy transfer, *J. Biochem. Biophys. Methods* 19:259–274.
61. Tweet, A. G., Bellamy, W. D., and Gaines, G. L., 1964, Fluorescence quenching and energy transfer in monomolecular films containing chlorophyll, *J. Chem. Phys.* 41:2068–2077.
62. Loura, L. M. S., Fedorov, A., and Prieto, M., 1996, Resonance energy transfer in a model system of membranes: Application to gel and liquid crystalline phases, *Biophys. J.* 71:1823–1836.
63. Stryer, L. (ed.), 1995, *Biochemistry*, 4th ed., W. H. Freeman and Company, New York. (See p. 274.)
64. Wang, S., Martin, E., Cimino, J., Omann, G., and Glaser, M., 1988, Distribution of phospholipids around gramicidin and D-β-hydroxybutyrate dehydrogenase as measured by resonance energy transfer, *Biochemistry* 27:2033–2039.
65. Shahrokh, Z., Verkman, A. S., and Shohet, S. B., 1991, Distance between skeletal protein 4.1 and the erythrocyte membrane bilayer measured by resonance energy transfer, *J. Biol. Chem.* 266:12082–12089.
66. McCallum, C. D., Su, B., Neuenschwander, P. F., Morrissey, J. H., and Johnson, A. E., 1997, Tissue factor positions and maintains the factor VIIa active site far above the membrane surface even in the absence of the factor VIIa Gla domain, *J. Biol. Chem.* 272:30160–30166.
67. Davenport, L., Dale, R. E., Bisby, R. H., and Cundall, R. B., 1985, Transverse location of the fluorescent probe 1,6-diphenyl-1,3,5-hexatriene in model lipid bilayer membrane systems by resonance excitation energy transfer, *Biochemistry* 24:4097–4108.
68. Wolf, D. E., Winiski, A. P., Ting, A. E., Bocian, K. M., and Pagano, R. E., 1992, Determination of the transbilayer distribution of fluorescent lipid analogues by nonradiative fluorescence resonance energy transfer, *Biochemistry* 31:2865–2873.
69. Isaacs, B. S., Husten, E. J., Esmon, C. T., and Johnson, A. E., 1986, A domain of membrane-bound blood coagulation factor Va is located far from the phospholipid surface. A fluorescence energy transfer measurement, *Biochemistry* 25:4958–4969.
70. Ladokhin, A. S., Wimley, W. C., Hristova, K., and White, S. H., 1997, Mechanism of leakage of contents of membrane vesicles determined by fluorescence requenching, *Methods Enzymol.* 278:474–486.
71. Kok, J. W., and Hoekstra, D., 1993, Fluorescent lipid analogues applications in cell and membrane biology, *Fluorescent and Luminescent Probes for Biological Activity*, W. T. Mason (ed.), Academic Press, New York, pp. 101–119.
72. Pyror, C., Bridge, M., and Loew, L. M., 1985, Aggregation, lipid exchange, and metastable phases of dimyristoylphosphatidylethanolamine vesicles, *Biochemistry* 24:2203–2209.
73. Duzgunes, N., and Bentz, J., 1988, in *Spectroscopic Membrane Probes*, L. D. Loew (ed.), CRC Press, Boca Raton, Florida, pp. 117–159.
74. Silvius, J. R., and Zuckermann, M. J., 1993, Interbilayer transfer of phospholipid-anchored macromolecules via monomer diffusion, *Biochemistry* 32:3153–3161.
75. Bennett, R. G., 1964, Radiationless intermolecular energy transfer. I. Singlet–singlet transfer, *J. Chem. Phys.* 41:3037–3041.
76. Eisenthal, K. B., and Siegel, S., 1964, Influence of resonance transfer on luminescence decay, *J. Chem. Phys.* 41:652–655.
77. Birks, J. B., and Georghiou, S., 1968, Energy transfer in organic systems VII. Effect of diffusion on fluorescence decay, *Proc. R. Soc. (J. Phys. B)* 1:958–965.
78. Thomas, D. D., Caslsen, W. F., and Stryer, L., 1978, Fluorescence energy transfer in the rapid diffusion limit, *Proc. Natl. Acad. Sci. U.S.A.* 75:5746–5750.
79. Selvin, P. R., Rana, T. M., and Hearst, J. E., 1994, Luminescence resonance energy transfer, *J. Am. Chem. Soc.* 116:6029–6030.
80. Li, M., and Selvin, P. R., 1995, Luminescent polyaminocarboxylate chelates of terbium and europium: The effects of chelate structure, *J. Am. Chem. Soc.* 117:8132–8138.
81. Berlman, I. B., 1973, *Energy Transfer Parameters of Aromatic Compounds*, Academic Press, New York.
82. Fairclough, R. H., and Cantor, C. R., 1978, The use of singlet energy transfer to study macromolecular assemblies, *Methods Enzymol.* 48:347–379.
83. Mathis, G., 1993, Rare earth cryptates and homogeneous fluoroimmunoassays with human sera, *Clin. Chem.* 39:1953–1959.

84. Lakowicz, J. R., Johnson, M. L., Wiczk, W., Bhat, A., and Steiner, R. F., 1987, Resolution of a distribution of distances by fluorescence energy transfer and frequency-domain fluorometry, *Chem. Phys. Lett.* **138**:587–593.

PROBLEMS

13.1. *Calculation of a Distance from the Transfer Efficiency*: Use the emission spectra in Figure 13.29 to calculate the distance from the indole donor to the dansyl acceptor. Assume that there is a single D–A distance and that diffusion does not occur during the donor excited-state lifetime. The Förster distance $R_0 = 25.9$ Å, and the donor-alone lifetime is 6.8 ns. What is the D–A distance? What is the donor lifetime in the TUD D–A pair?

13.2. *Measurement of RET Efficiencies (E) from Fluorescence Intensities and Lifetimes*: Use Eq. [13.11] to derive the expressions for E based on intensities (Eq. [13.14]) or lifetimes (Eq. [13.13]).

13.3. *Distance Dependence of Energy Transfer*: The theory of Förster states that the rate of energy transfer depends on $1/r^6$, where r is the donor-to-acceptor distance. This prediction was tested experimentally using naphthyl donors and dansyl acceptors linked by rigid polyprolyl spacers (Figure 13.30). Figure 13.31 shows the excitation spectra for this series of D–A pairs. Assume that each polyprolyl spacer contributes 2.83 Å to the spacing and that the D–A distance ranges from 12 Å ($n = 1$) to 46 Å ($n = 12$).

Use the excitation spectra to demonstrate that k_T depends on $1/r^6$. Note that the dansyl acceptor absorbs maximally at 340 nm and the naphthyl donor has an absorption maximum at 290 nm. Excitation spectra were recorded with the emission monochromator centered on the dansyl emission near 450 nm. What is R_0 for this D–A pair?

13.4. *Effect of Spectral Overlap on the Rate of Energy Transfer*: Haugland *et al.*[18] investigated the effect of the magnitude of the spectral overlap integral on the rate of fluorescence energy transfer. For this study, they employed the steroids shown in Figure 13.32. They measured the fluorescence lifetimes of compounds I and II. The indole moiety is the donor which transfers energy to the ketone acceptor. Both the absorption spectrum of the ketone and the emission

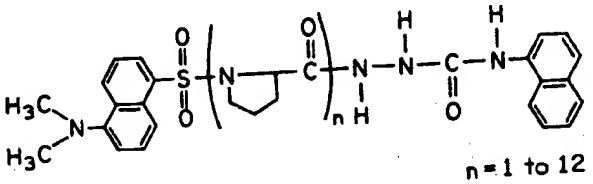

Figure 13.30. Structure of dansyl-(L-prolyl)$_n$-α-naphthyl used for determining the effects of distance on energy transfer. Revised from Ref. 14.

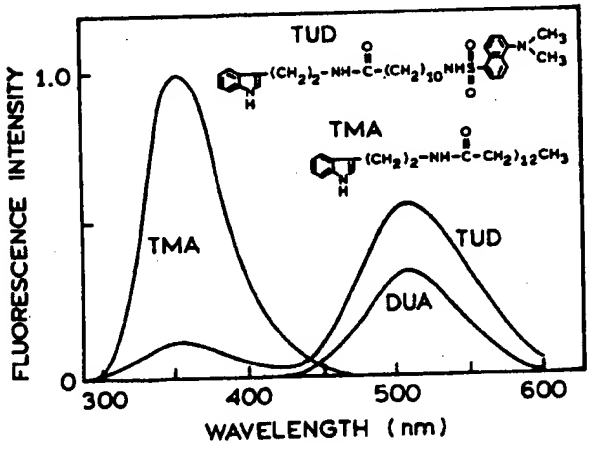

Figure 13.29. Emission spectra of a donor control (TMA) and a donor–acceptor pair (TUD) in propylene glycol at 20 °C. DUA is a dansyl-labeled fatty acid, which is the acceptor-only control sample. Revised from Ref. 84.

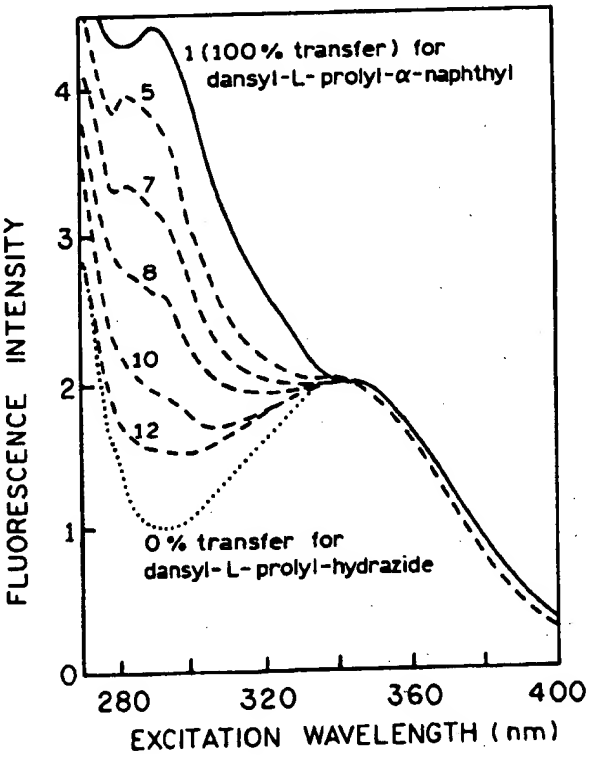

Figure 13.31. Excitation spectra of dansyl-(L-prolyl)$_n$-α-naphthyl molecules. Spectra are shown for dansyl-L-prolyl-hydrazide (···), dansyl-L-prolyl-α-naphthyl (———), and dansyl-(L-prolyl)$_n$-α-naphthyl (— — —), $n = 5$, 7, 8, 10, and 12. Emission was detected at the dansyl emission maximum near 450 nm. Revised from Ref. 16.

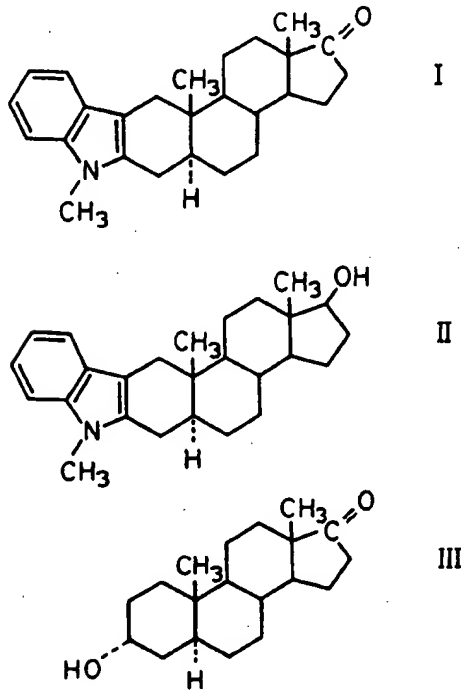

Figure 13.32. Structure of the rigid steroid donor-acceptor pair (I), the steroid containing the donor alone (II), and the steroid containing the acceptor alone (III). Indole is the donor and the carbonyl group is the acceptor. Revised from Ref. 18.

Table 13.5. Fluorescence Spectral Properties of Compounds I and II in a Series of Solvents[a]

Solvent	τ (ns) I	τ (ns) II	n_d	J (cm^6/mmol × 10^{19})
Methanol	5.3	5.6	1.331	1.5
Ethanol	5.6	6.5	1.362	3.0
Dioxane	3.6	5.4	1.423	13.0
Ethyl acetate	3.3	4.7	1.372	12.8
Ethyl ether	2.1	4.5	1.349	30.0
Heptane	1.1	2.8	1.387	60.3

[a]From Ref. 18.

spectrum of the indole are solvent-sensitive. Specifically, the emission spectrum of the indole shifts to shorter wavelengths and the absorption spectrum of the ketone shifts to longer wavelengths as the solvent polarity decreases (Figure 13.33). These shifts result in increasing spectral overlap with decreasing solvent polarity.

Use the data in Table 13.5 to demonstrate that k_T is proportional to the first power of the extent of spectral overlap (J).

13.5. *Calculation of a Förster Distance*: Calculate the Förster distance for the tryptophan-to-dansyl donor–acceptor pair shown in Figure 13.8. The quantum yield of the donor is 0.21.

13.6. *Optical Assay for cAMP*: The effect of cAMP on the donor- and acceptor-labeled protein kinase (Figure 13.15) suggests its use for measuring cAMP. Derive an expres-

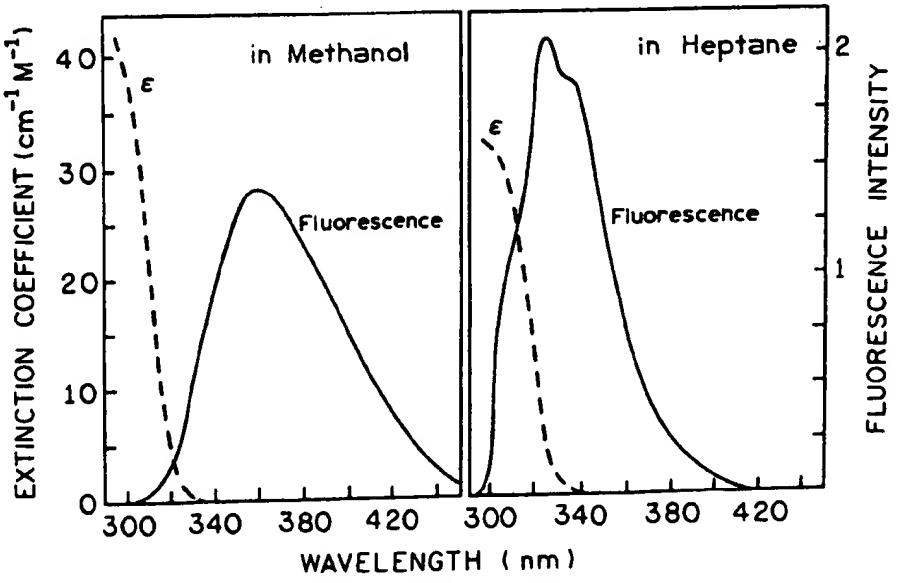

Figure 13.33. Overlap of emission spectrum of the indole donor (II) with the absorption spectrum of the carbonyl acceptor (III). Revised from Ref. 18.

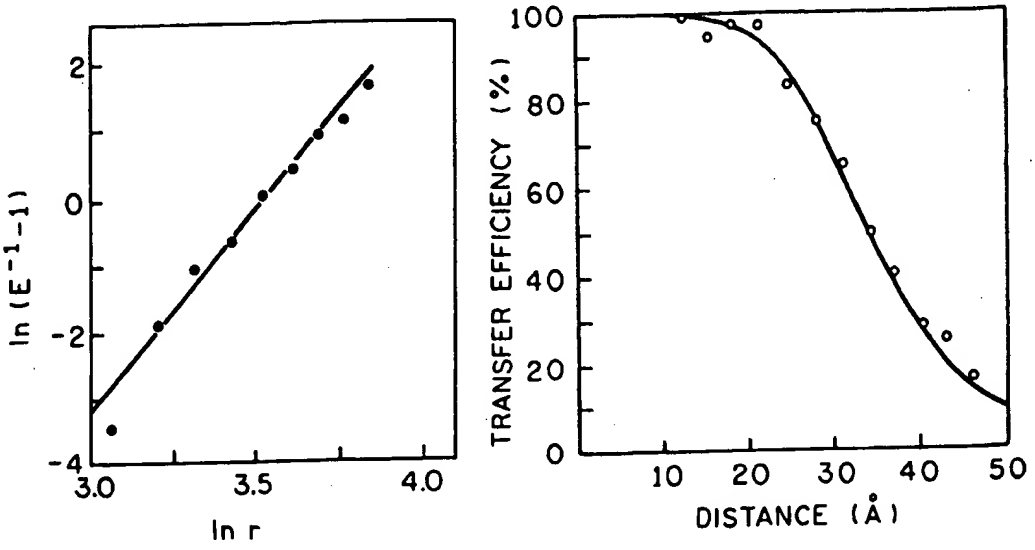

Figure 13.34. Distance dependence of the energy transfer efficiencies in dansyl-(L-propyl)$_n$-α-naphthyl, n = 1–12. Revised from Ref. 16.

sion relating the ratio of donor to acceptor intensities to the protein kinase–cAMP dissociation constant. Assume that the donor and acceptor quantum yields are unchanged upon binding of cAMP, except for the change in energy transfer. Explain any advantages of an assay based on intensity ratios rather than direct intensity measurements.

13.7. *Characteristics of a Closely Spaced D–A Pair.* Assume that you have isolated a protein which contains a single tryptophan residue and binds dinitrophenol (DNP) in the active site. The absorption spectrum of DNP overlaps with the emission spectrum of the tryptophan residue. Assume R_0 = 50 Å and that DNP is not fluorescent. The fluorescence intensities of the tryptophan residue are 20.5 and 4.1 in the absence and presence of DNP, respectively, after correction for the inner filter effects due to the DNP absorption.

A. What is the energy transfer efficiency?
B. Assume that the unquenched lifetime is 5 ns. What is the expected lifetime in the presence of DNP?
C. What is the energy transfer rate?
D. What is the distance between the tryptophan and the DNP?
E. Assume that the solution conditions change so that the distance between the tryptophan and the DNP is 20 Å. What is the expected intensity for the tryptophan fluorescence?
F. For this same solution (r = 20 Å), what would be the effect on the fluorescence intensity of a 1% impurity of a second protein which did not bind DNP? Assume that this second protein has the same lifetime and quantum yield as the protein under investigation.
G. What lifetime would you expect for the sample which contains the impurity? Would this lifetime provide any indication of the presence of an impurity?

13.8. *Effect of κ^2 on the Range of Possible Distances:* Suppose you have a donor- and acceptor-labeled protein which displays the following steady-state anisotropies:

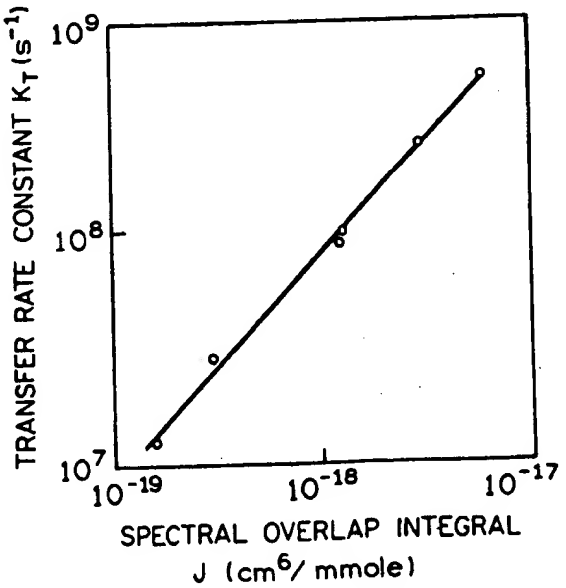

Figure 13.35. Dependence of the rate of energy transfer on the magnitude of the overlap integral. Revised from Ref. 18.

Fluorophore	τ (ns)	r_D or r_A	r_0
Donor-alone control	5	0.1	0.4
Acceptor	15	0.05	0.4

Using an assumed value of $\kappa^2 = \frac{2}{3}$, the D–A distance was calculated to be 25 Å. R_0 is also equal to 25 Å. Assume that the protein displays a rotational correlation time of 5 ns. Use the data provided to calculate the range of distances possible for the D–A pair.

13.9. *Effect of Acceptor Underlabeling on the Calculated Transfer Efficiency*: Suppose that you have a presumed D–A pair. In the absence of acceptor, the donor displays a steady-state intensity $F_D = 1.0$, and in the presence of acceptor, $F_{DA} = 0.5$. Calculate the transfer efficiency assuming that the fractional labeling with acceptor (f_A) is 1.0 or 0.5. How does the change in f_A affect the calculated distance?

13.10. *FRET Efficiency from the Acceptor Intensities*: Derive Eq. [13.25] for the case in which donor labeling is complete; $f_D = 1.0$. Also derive Eq. [13.25] for the case in which donor labeling is incomplete ($f_D < 1$).

13.11. *Correction for Overlapping Donor and Acceptor Emission Spectra*: Equation [13.25] does not consider the possible contribution of the donor emission at the wavelength used to measure acceptor fluorescence (λ_A). Derive an expression for the enhanced acceptor fluorescence when the donor emits at λ_A. Explain how the apparent transfer efficiency, calculated without consideration of the donor contribution, would be related to the true transfer efficiency.

13.12. *Effect of non-RET quenching:* Suppose that you have a protein with a single tryptophan residue. Assume also that the protein noncovalently binds a ligand which serves as a RET acceptor for the tryptophan residue and that the acceptor site is allosterically linked to the donor site such that acceptor binding induces an additional rate of donor quenching, k_q, in addition to k_T.

What is the apparent transfer efficiency upon acceptor binding in terms of τ_D, k_T, and k_q? Is the apparent value (E_D) smaller or larger than the true value (E)?